Developmental constraints on genome evolution in four bilaterian model species

Jialin Jiu[1,2], Marc Robinson-Rechavi[1,2*]

1 Department of Ecology and Evolution, University of Lausanne, Switzerland

2 Swiss Institute of Bioinformatics, Lausanne 1015, Switzerland

* corresponding author: marc.robinson-rechavi@unil.ch

Abstract

Developmental constraints on genome evolution have been suggested to follow either an early conservation model or an "hourglass" model. Both models agree that late development strongly diverges between species, but debate on which developmental period is the most conserved. Here, based on a modified "Transcriptome Age Index" approach, i.e. weighting parameters by expression level, we analyzed the constraints acting on three evolutionary traits of protein coding genes (strength of purifying selection on protein sequences, phyletic age, and duplicability) in four species: nematode worm *C. elegans*, fly *D. melanogaster*, zebrafish *D. rerio*, and mouse *M. musculus*. In general, we found that both models can be supported by different genomic properties. The evolution of phyletic age and of duplicability follow an early conservation model in all species, but sequence evolution follows different models in different species: an early conservation model in fly, and an hourglass model in both zebrafish and mouse. Further analyses indicate that stronger purifying selection on sequences in early development of fly and during the morphological 'phylotypic' period of zebrafish and mouse are driven by temporal pleiotropy of these genes. In addition, we report evidence that expression in late development is enriched with retrogenes, which usually lack efficient regulatory elements. This implies that expression in late development could facilitate transcription of new genes, and provide opportunities for acquisition of function. Finally, in nematode, we suggest that dosage imbalance could be one of the main factors that cause depleted expression of high duplicability genes in early development.

Introduction

Evolutionary changes in the genome can cause changes in development, which are subject to natural selection. This leads developmental processes to constrain genome evolution. More precisely, selection on the output of development affects evolution of the genomic elements active in development. Currently, based on morphological similarities during development, two popular models have been proposed to bridge developmental and evolutionary biology. The early conservation model, modified from the “third law” of Von Baer (1828) (as cited in Kalinka and Tomancak 2012), suggests that the highest morphological similarities among species from the same phylum occur in early development, followed by a progressive evolutionary divergence over ontogeny. It should be noted that Von Baer in fact based his observations on post-gastrulation embryos (Kalinka and Tomancak 2012; Abzhanov 2013). The "developmental burden" concept was proposed to explain this model. It suggested that the development of later stages is dependent on earlier stages, so that higher conservation should be found in the earlier stages of development (Garstang 1922; Riedl 1978) (as discussed in Irie and Kuratani 2014). Based on renewed observations in modern times, however, Duboule (1994) and Raff (1996) proposed the developmental "hourglass model". This model suggested that a "phylotypic period" (Richardson 1995) in middle development has higher morphological similarities than early or late development. Several mechanisms have been proposed to explain this observation. Duboule (1994) proposed that it may be due to co-linear Hox cluster gene expression in time and space. Raff (1996) suggested a high inter-dependence in signaling among developmental modules in middle development. Galis and Metz (2001) also highlighted the high number of interactions at this period, although Comte et al. (2010) did not find any molecular evidence for these interactions. It is worth noting that the hourglass model was not supported by a comprehensive study of vertebrate embryonic morphology variation (Bininda-Emonds et al. 2003). A number of alternatives have been proposed, for example the “adaptive penetrance model” (Richardson et al. 1997) and the “ontogenetic adjacency model” (Poe and Wake 2004). Of note, the higher divergence of late development could also be due to stronger adaptive selection, the "Darwin hypothesis" (Artieri et al. 2009). This question is independent of the pattern of constraints (early or hourglass)

which are the focus of this study, and we explore it in a companion study (Liu and Robinson-Rechavi 2017).

Both main models have been supported by recent genomic level studies based on different properties (such as expression divergence, sequence divergence, duplication, or phyletic age), different species, and different analysis methods. Concerning expression divergence, interestingly, all studies are consistent across different species and research groups (Kalinka et al. 2010; Irie and Kuratani 2011; Yanai et al. 2011; Levin et al. 2012; Wang et al. 2013; Gerstein et al. 2014; Ninova et al. 2014; Zalts et al. 2017). All of them suggested that middle development has the highest transcriptome conservation, i.e. the hourglass pattern. On the other hand, when animals are compared between different phyla, middle development appears to have the highest divergence (Levin et al. 2016) (but see (Dunn et al. 2018). From other properties, however, the results are inconclusive based on different methods (Castillo-Davis and Hartl 2002; Cutter and Ward 2005; Davis et al. 2005; Hazkani-Covo et al. 2005; Hanada et al. 2007; Irie and Sehara-Fujisawa 2007; Cruickshank and Wade 2008; Roux and Robinson-Rechavi 2008; Artieri et al. 2009; Domazet-Loso and Tautz 2010; Quint et al. 2012; Piasecka et al. 2013; Cheng et al. 2015; Drost et al. 2015).

Generally, the methods used to measure developmental constraints at the genomic level can be divided into three categories: proportion based analysis, module analysis, and transcriptome index analysis.

Proportion based analysis consists in testing the proportion of genes with a given property within all expressed genes (Roux and Robinson-Rechavi 2008). The method is less used following the emergence of accurate transcriptome-scale data, since it does not take into account the contributions of expression abundance.

Module analysis consists in studying evolutionary properties of distinct sets of genes (modules) which are specifically expressed in groups of developmental stages (Piasecka et al. 2013). This method can avoid problems caused by genes expressed over all or a large part of development. For example, trends might be diluted by

highly expressed housekeeping genes, which contribute to the average expression at all developmental stages. However, this approach can only measure the developmental constraints for a specific subset of genes, instead of considering the composition of the whole transcriptome.

Transcriptome index analysis is a weighted mean: the mean value of an evolutionary parameter is weighted by each gene's expression level (Domazet-Loso and Tautz 2010). This method has the benefit of detecting evolutionary constraints on the whole transcriptome, but patterns can be driven by a subset of very highly expressed genes, or even by a few outliers, because the difference between highly and lowly expressed genes can span several orders of magnitude. For instance, Domazet-Loso and Tautz (2010) reported that transcriptomes of middle development stages of *D. rerio* have a higher proportion of old genes than transcriptomes of early and late development stages, using the transcriptome age index. However, Piasecka et al. (2013) re-analyzed the same data and reported that the highest proportion of old genes was in transcriptomes of early development stages, once a standard log-transformation of microarray signal intensities was done, a result confirmed by module analysis and proportion based analysis.

In addition, several statistical methods have been proposed to distinguish the hourglass model from the early conservation model.

The parabolic test is based on fitting both first degree and second degree polynomial models (Roux and Robinson-Rechavi 2008). The hourglass model is supported if the parabolic function provides a significantly better fit and its minimum corresponds to middle development. This method has been criticized for being too specific and insensitive to other non-parabolic hourglass patterns (Drost et al. 2015).

The flat line test simply tests whether variance of transcriptome indexes across development is significantly higher than variance from random samples (Domazet-Loso and Tautz 2010; Quint et al. 2012). But a significant difference does not necessarily imply the existence of an hourglass pattern (Drost et al. 2015).

Since these two methods are either too strict or without power to distinguish hourglass model, Drost et al. (2015) proposed a "reductive hourglass test" which focuses on testing the presence of an hourglass pattern of divergence: high-low-high. For this, development can be divided into three periods (early, phylotypic, and late), based on the known phylotypic period from morphological studies. Then, a permutation method is used to test whether the mean value in the phylotypic period is significantly lower than in early and late periods.

Overall, the transcriptome index analysis should be the best method to measure developmental constraints on the whole transcriptome, if care is taken to properly treat the expression values. Moreover, the reductive hourglass test should be used to objectively test the hourglass model, alone or in combination with other methods.

Because previous studies used different methodologies, and few studies adopted a transformed transcriptome index analysis, their conclusions cannot be compared consistently, making a biological conclusion concerning developmental constraints across species and features difficult. What's more, while many studies focus on distinguishing between early conservation model and hourglass conservation model, we still know very little of the factors driving these patterns.

To measure developmental constraints on genome evolution, we calculated transcriptome indexes over the development of four species (*C. elegans, D. melanogaster, D. rerio* and *M. musculus*), for three evolutionary parameters (strength of purifying selection on coding sequences (ω_0), phyletic age, and duplicability (paralog number)), with three transformations of expression values (non-transformed, $\log_2$ transformed, and square root transformed). For *C. elegans*, the strength of purifying selection on coding sequences was not reliably estimated, with no data in the Selectome database (Moretti et al. 2014) and very high values of estimated synonymous distances (dS) from Ensembl Metazoa (Kersey et al. 2016) (Figure S1); thus we did not include this parameter in the study of *C. elegans*. In general, we found results consistent with early conservation for phyletic age and paralog number in the four species, but different models for sequence evolution in different phyla. In addition, $\log_2$ transformed transcriptome indexes are always consistent with square

root transformed transcriptome indexes but not with non-transformed transcriptome indexes.

Results and discussion

Effect of expression value transformation on transcriptome indexes

As mentioned in the Introduction, the pattern from a transcriptome index analysis may not reflect the global behavior of the transcriptome, but that of a small fraction of very highly expressed genes, or even of a few outliers. In order to systematically test this issue, we calculated 95% confidence intervals of transcriptome indexes based on $\log_2$ transformed, square root transformed, and non-transformed expression values (see Methods). Then, for the purpose of comparing the range of confidence intervals in the same scale, we plotted the ratio of upper to lower confidence interval boundary across development. Clearly, at a given confidence level (95% here), we can see that the ratio of non-transformed transcriptome indexes is much higher and more variable than transformed transcriptome indexes, indicating that the transcriptome indexes estimated from transformed expression are more stable. The most stable pattern comes from $\log_2$ transformed transcriptome indexes, although it is quite similar with square root transformation. We note that while log-transformation is routine in most application of transcriptomics, many analyses of "hourglass" patterns use non transformed expression data.

In summary, although a subset of genes with dramatically different expression values in different stages could be interesting in some sense, when the goal is to investigate the general tendency of the transcriptome, log-transformation for expression value is necessary and efficient to reach a stable estimation.

Variation of evolutionary transcriptome indexes across development

Here, based on $\log_2$ transformed expression values, we calculated transcriptome indexes for strength of purifying selection on coding sequences (ω_0), phyletic age, and duplicability (paralog number). In order to objectively distinguish the hourglass model from the early conservation model, we used a permutation test method similar to that of Drost et al. (2015) (see Methods). For all parameters considered the highest

divergence is observed in late development. Thus a significant *p*-value for lower divergence in middle *vs*. early development supports the hourglass model, whereas a lack of significance supports the early conservation model. We consider early conservation to cover both stronger conservation in early than middle development, and similar strong conservation over early and middle development, and hence we use a one-sided test.

For the transcriptome indexes of phyletic age (Transcriptome Age Index: TAI) and of paralog number (Transcriptome Paralog Index: TPI), in all four species, we observed that genes with higher duplicability and younger phyletic age trend to be expressed at later developmental stages, which corresponds to early conservation (Figure 2). For the transcriptome index of purifying selection on coding sequence (Transcriptome Divergence Index: TDI), we observed different patterns in different species (Figure 2). In *D. melanogaster,* there is an early conservation pattern of TDI: similar low TDI in early and middle development, high TDI in late development. In *D. rerio* and *M. musculus,* however, there is an hourglass pattern of TDI: medium TDI in early development, low TDI in middle development, and high TDI in late development. In addition, we also repeated these analyses based on square root transformed expression values (Figure S2) and on non-transformed expression values (Figure S3). In general, the results from square root transformation are highly consistent with from $\log_2$ transformation, but not with from non-transformation. For example, with non-transformed expression data, the TDI in *D. melanogaster* and the TAI in *D. rerio* changed from early conservation to hourglass patterns. Of note, in *M. musculus*, since there is only one early development stage, the results reported here should be regarded rather as indicative.

In *D. melanogaster*, we did not confirm the results of Drost et al. (2015) for either phyletic age or sequence evolution. For TAI, after $\log_2$ transformation of expression data, we found an early conservation pattern instead of the hourglass pattern which they reported (Figure S4B). It appears that the hourglass pattern of phyletic age in their study is driven by a few highly expressed genes, consistently with our previous observations in *D. rerio* (Piasecka et al. 2013). This is verified by excluding the top 10% most expressed genes and analyzing without transformation (Figure S4C). Of

note, that phyletic age hourglass with uncorrected expression was also reported earlier (Domazet-Loso and Tautz 2010). For TDI, the different patterns could be in part due to distinct measurements of sequence evolution: Drost et al. (2015) analyzed discrete sequence divergence strata, whereas we used continuous values.

Overall, these results suggest that genes under strong purifying selection on their protein sequence trend to be expressed in early development in *D. melanogaster*, but in middle development for two vertebrates; it remains to be seen how much these observations extend to more arthropods or chordates. They also extend our previous observations that genes expressed earlier have a lower duplicability and an older age (Roux and Robinson-Rechavi 2008; Piasecka et al. 2013). In addition, it poses the question whether a pattern driven by the minority of very highly expressed genes is relevant to understanding Evo-Devo, which is generally driven by lowly expressed genes such as transcription factors.

Expression of temporal pleiotropy genes across development

Several models have been proposed to explain why some developmental stages are more conserved than others, as presented in the Introduction. In all models, a common point is that high conservation is caused by selection against deleterious pleiotropic effects of mutations. This implies that higher sequence conservation in early or middle developmental stages is caused by higher pleiotropy of genes expressed in these stages, pleiotropy being one of the major factors that constrain sequence evolution (Fraser et al. 2002).

In order to test this hypothesis, we used one type of development related pleiotropic effect: temporal pleiotropy (Artieri et al. 2009) (expression breadth across development). This is similar to spatial pleiotropy (Larracuente et al. 2008; Kryuchkova-Mostacci and Robinson-Rechavi 2015) (expression breadth across tissues) or connective pleiotropy (Fraser et al. 2002) (protein-protein connectivity). The more stages a gene is expressed in, the more traits it could affect, so it is expected to be under stronger evolutionary constraints (Wagner and Zhang 2011). For *D. melanogaster* and *C. elegans*, we defined FPKM>1 as expressed. For *D. rerio* and *M. musculus,* we set genes with microarray signal rank in top 70% as expressed.

We calculated the proportion of potentially pleiotropic genes as expressed in more than 50% of development stages. We found pleiotropic genes enriched in the middle development of *C. elegans, D. rerio* and *M. musculus*, but in both early and middle development of *D. melanogaster* (Figure 3). We also found similar patterns when we define pleiotropic genes as expressed in more than 70% of development stages (Figure S5). Since the late development of *C. elegans* and *D. melanogaster* can clearly be divided into two periods with distinct patterns, we removed the second period of late development, and found the same overall trend (Figure S6). For *D. rerio* and *M. musculus*, in addition, we observed consistent results based on setting expressed genes as microarray signal rank in the top 90% or 50% (Figure S7, S8). Because RNA-seq is more efficient to detect specifically expressed genes than microarrays (Kryuchkova-Mostacci and Robinson-Rechavi 2016a), for both *C. elegans* and *D. melanogaster* with RNA-seq data, we also calculated a stage specificity index (Tau) of gene expression, based on the tissue specificity index (Yanai et al. 2005; Kryuchkova-Mostacci and Robinson-Rechavi 2016a). Genes with lower Tau are expressed across more developmental stages with little variation in level of expression. With a transcriptome index of Tau (Transcriptome Tau Index: TTI), we observed very similar results as well (Figure S9). Similar observations of higher temporal pleiotropy for genes in middle development in vertebrates were recently reported by Hu et al. (2017).

Based on these observations, we further checked whether higher temporal pleiotropic constraint could explain stronger purifying selection on sequence evolution. As expected, we found that pleiotropic genes have lower ω_0 than non-pleiotropic genes (Figure S10). Thus, we re-calculated TDI separately for pleiotropic genes and for non-pleiotropic genes. Interestingly, the global pattern appears to be driven by the pleiotropic genes (Figure 4): early conservation for *D. melanogaster*, and hourglass for *D. rerio* and *M. musculus*.

In summary, it seems that development stages with a higher proportion of broadly expressed genes are under stronger pleiotropic constraint on sequence evolution. And

thus, that different sequence constraint patterns in different species are driven by different distributions of pleiotropic genes.

Higher expression of retrogenes in later development stages

In adult anatomy, young genes are mainly enriched for expression in testis (Kaessmann 2010). Two main factors have been proposed to explain this pattern. Firstly, permissive chromatin in testis facilitates the transcription of new genes (Soumillon et al. 2013). Secondly, as the most rapidly evolving organ at genomic level, there is least purifying selection acting on new genes expressed in testis (Kaessmann 2010). Is there a similar explanation for the ontogenic pattern of young genes tending to be expressed in late development stages? As testis constitutes the most rapidly evolving organ transcriptome, late development represents the most rapidly evolving stage transcriptome, owing to both relaxed purifying selection (Artieri et al. 2009) and to increased positive selection (Liu and Robinson-Rechavi 2017). Thus, we suggest that expression in late development might, like in testis, promote the fixation and functional evolution of new genes.

In order to test this, we analyzed the expression of retrogenes across development. Since retrogenes usually lack regulatory elements, most of them fail to acquire transcription and achieve function (Kaessmann et al. 2009). So, if late development, like testis, can facilitate the transcription of new genes, promoting their fixation, we should observe higher expression of retrogenes in later developmental stages. To display the expression variation of retrogenes across development, we fitted polynomial models of the first degree and of the second degree. We kept the second degree polynomial model (parabola) only if it provided a significantly better fit (tested with ANOVA, $p<0.05$). Since the development time points in *M. musculus* transcriptome data set are close to uniformly sampled, we used the natural scale of development time for regression. For *C. elegans*, *D. melanogaster* and *D. rerio*, however, we used the logarithmic scale, to limit the effect of post-embryonic time points. Because retrogenes have higher expression in testis, and testis is already differentiated after middle development, we excluded testis genes in our analyses for *D. melanogaster* and *M. musculus,* where the information of testis gene expression was available. We found that the median expression of retrogenes is at its maximum

in late development (Figure 5), even though the specific patterns are different in different species: in *C. elegans*, the median expression progressively increases; in *D. melanogaster*, all the median values are 0 until stage 4 days, and then it progressively increases; in *D. rerio*, the median expression keeps increasing until stage 14 days, and then gradually decreases; in *M. musculus*, the median expression resembles an hourglass like pattern, but late development has much higher expression than either early or middle development.

These results confirm that late development could allow more transcription of newly originated gene copies, which usually lack efficient regulatory elements and transcriptional activity. Since the first step to functionality is acquiring transcription, we suggest that the functional acquisition and survival at the beginning of life history for new genes could be promoted by expression in late development. When beneficial mutations come, a subset of these new gene candidates could subsequently obtain adaptive functions in late development and evolve efficient regulatory elements and finally be retained long term in the genome. Thus, the higher proportion of young genes expressed in later development stages can be in part explained by these stages favoring the fixation of new genes.

Connectivity and dosage imbalance

It has previously been found that, in both *S. cerevisiae* and *C. elegans*, gene duplicability is negatively correlated with protein connectivity (Hughes and Friedman 2005; Prachumwat and Li 2006) which might be explained by dosage balance (Veitia 2002; Papp et al. 2003). Firstly, we checked the relationship of connectivity and duplicability in our datasets. We found, indeed, a negative relationship in *C. elegans* (Figure S11). In *D. melanogaster* and in *D. rerio*, there is a non-monotonous pattern (increasing first, and then decreasing), but the overall trend is more connectivity with less duplicability. In *M. musculus*, however, we did not observe a significant relationship between connectivity and duplicability. Secondly, we calculated a transcriptome index of connectivity (Transcriptome Connectivity Index: TCI). In *C. elegans*, earlier developmental stages have higher TCI, which means these stages trend to have higher expression of more connected genes (Figure 6). In *D. melanogaster*, we observed a similar pattern even though there is a trend of increased

TCI in Pupae stages. In *D. rerio*, however, there is a non-significant hourglass like pattern. In *M. musculus*, although we detected a significant hourglass pattern, the result reported here should be regarded rather as indicative since there is only one stage in early development. Thus, we hesitate to over interpret the result as evidence to support the hypothesis of a high number of interactions in vertebrate middle development (Raff 1996; Galis and Metz 2001).

These results indicate that, in *C. elegans*, earlier stages trend to express higher connectivity genes, which are less duplicable because more sensitive to dosage imbalance, but that this cannot be generalized to other animals. Of course, this is not exclusive with an adaptive scenario that early stages lack opportunities for neo- or sub-functionalization, because of simpler anatomical structures, which could also diminish fixation of duplicates in early development.

Conclusion

Our results concern both patterns and processes of evolution over development. For patterns, we tested the early conservation and hourglass models by using three evolutionary properties: strength of purifying selection, phyletic age and duplicability. Both duplicability and phyletic age support the early conservation model. Less duplicated genes and phyletically older genes are more expressed at earlier stages. The strength of purifying selection on protein sequence supports the early conservation model in *D. melanogaster* but the hourglass model in the vertebrates *D. rerio* and *M. musculus*.

For processes, we investigated the potential causes of the observed patterns. The different models of sequence evolution in different species appear to be driven by temporal pleiotropy of gene expression, since temporal pleiotropic genes are enriched in the early development of *D. melanogaster* but in the middle development of *D. rerio* and *M. musculus*. The enrichment in young phyletic age genes in late development might be related to a testis-like role of late development that facilitates the expression of retrogenes. Finally, in *C. elegans*, connectivity appears to be the main force explaining higher duplicability of genes expressed in later development.

Materials and Methods

Data files and analysis scripts are available on our GitHub repository: https://github.com/ljljolinq1010/developmental_constraints_genome_evolution

Expression data sets

For *D. rerio*, we used the processed microarray data (log-transformed and normalized) from our previous study (Piasecka et al. 2013). This data originally comes from (Domazet-Loso and Tautz 2010), which includes 60 stages from egg to adult. We further generated square root transformed and non-transformed expression values.

For *M. musculus*, the processed microarray data (log-transformed and normalized) was retrieved from Bgee (release 13.1, July 2015; Bastian et al., 2008), a database for gene expression evolution. This data includes eight stages from Theiler 11 to Theiler 26, and originally comes from (Irie and Kuratani 2011). We further generated square root transformed and non-transformed expression values.

For *D. melanogaster* and *C. elegans*, we obtained processed (non-transformed but normalized) RNA-seq data from http://www.stat.ucla.edu/~jingyi.li/software-and-data.html (Li et al. 2014), which originally comes from (Gerstein et al. 2010; Graveley et al. 2011). The *D. melanogaster* data set covers embryo, larva, pupae and adult, including 27 stages. The *C. elegans* data set covers 30 stages from embryo to larval and to adult. We further generated log-transformed and square root transformed expression values. For log-transformation, all the genes with RPKM <=1 were set as not expressed (Kryuchkova-Mostacci and Robinson-Rechavi 2016b), replaced by 1.0001 (this value is smaller than the smallest value of expressed genes), and $\log_2$ transformed.

For all data sets, we removed stages which precede the maternal to zygote transition (MZT) because these data sets are dominated by maternal transcripts (Tadros and Lipshitz 2009). In addition, we also excluded all adult stages, because we are focusing on developmental processes.

Omega0 (ω_0)

The ω_0 values were downloaded from Selectome (Moretti et al. 2014), a database of positive selection based on branch-site model (Zhang et al. 2005). Selectome excludes ambiguously aligned regions before model fitting. Omega0 is the dN/dS ratio (dN is the rate of non-synonymous substitutions, dS is the rate of synonymous substitutions) of the subset of codons which have evolved under purifying selection according to the branch-site model. We used ω_0 from the Clupeocephala branch, the Murinae branch, and the Melanogaster group branch for *D. rerio*, *M. musculus*, and *D. melanogaster*, respectively. One gene could have two ω_0 values in the focal branch because of duplication events. In this case, we keep the value of the branch following the duplication and exclude the value of the branch preceding the duplication.

phyletic age data

Phyletic ages were retrieved from Ensembl version 84 (Yates et al. 2016) using the Perl API. For each gene, we browsed its gene tree from the root and dated it by the first appearance. We assigned the oldest genes with phyletic age value of 1 and the youngest genes with the highest phyletic age value. So, genes can be split into discrete "phylostrata" by phyletic age. We classified 3 phylostrata, 4 phylostrata, 9 phylostrata and 18 phylostrata respectively for *C. elegans*, *D. melanogaster*, *D. rerio* and *M. musculus*. The definition of phylostrata is dependent on the available genome sequences in related lineages, hence the differences between species.

Number of paralogs

We retrieved the number of paralogs from Ensembl release 84 (Yates et al. 2016) using BioMart (Kinsella et al. 2011).

Retrogene data

For *C. elegans,* we retrieved 33 retrogenes from (Zou et al. 2012). For *D. melanogaster,* we retrieved 72 retrogenes from retrogeneDB (Kabza et al. 2014). For *D. rerio* we retrieved 113 retrogenes from (Fu et al. 2010). For *M. musculus* we retrieved 268 retrogenes from retrogeneDB (Kabza et al. 2014).

Connectivity data

We retrieved connectivity (protein-protein interactions) data from the OGEE database (Chen et al. 2012).

Testis specific genes

Similar to the measure of stage specificity, we calculated tissue specificity for *M. musculus* and *D. melanogaster*. We retrieved processed RNA-seq data of 22 *M. musculus* tissues and 6 *D. melanogaster* tissues from (Kryuchkova-Mostacci and Robinson-Rechavi 2016b). We defined genes with highest expression in testis and with tissue specificity value ≥ 0.8 as testis specific genes.

Transcriptome index analysis for different evolutionary parameters

The TEI (transcriptome evolutionary index) is calculated as:

$$\mathrm{TEI}_s = \frac{\sum_{i=1}^{n} E_i e_{is}}{\sum_{i=1}^{n} e_{is}},$$

where s is the developmental stage, E_i is the relevant evolutionary parameter (ω_0, paralog number, phyletic age, stage specificity, or protein connectivity) of gene i, n is the total number of genes, and e_{is} is the expression level of gene i in developmental stage s; by default we use log-transformed expression levels for e_{is}.

Confidence interval analysis

Firstly, we randomly sampled gene IDs from original data set 10,000 times with replacement. Then, we computed transcriptome indexes for the 10,000 samples. Finally, the 95% confidence interval is defined as the range from quantile 2.5% to quantile 97.5% of the 10,000 transcriptome indexes. This approach was integrated into myTAI (Drost et al. 2016), a R package for evolutionary transcriptome index analysis.

Permutation test

We first assigned all development stages into three broad development periods (before phylotypic period, phylotypic period, and after phylotypic period) based on

previous defined phylotypic periods from morphological and genomic studies. For *C. elegans*, the phylotypic period is defined as the ventral enclosure stage (Levin et al. 2012); for *D. melanogaster*, the phylotypic period is defined as an extended germband stage (Sander 1983; Kalinka et al. 2010); for *D. rerio*, the phylotypic period is defined as the segmentation and pharyngula stages (Ballard 1981; Wolpert 1991; Slack et al. 1993; Domazet-Loso and Tautz 2010); for *M. musculus*, the phylotypic period is defined as Theiler stages 13 to 20 (Ballard 1981; Wolpert 1991; Slack et al. 1993; Irie and Kuratani 2011). Next, we calculated the difference of mean transcriptome indexes between the early module and the middle module ($\Delta e\text{-}m$). Then, we randomly sampled the values of the relevant parameter (ω_0, paralog number, phyletic age, stage specificity or protein connectivity) from the original data set 10,000 times without replacement. Finally, we approximated a normal distribution for $\Delta e\text{-}m$ based on 10,000 $\Delta e\text{-}m$ values computed from the permutated samples. The *p*-value of the hourglass model *vs*. the early conservation model for each parameter is the probability of a randomly sampled $\Delta e\text{-}m$ exceeding the observed $\Delta e\text{-}m$. For protein connectivity, the *p*-value of the hourglass model is the probability that a randomly sampled $\Delta e\text{-}m$ lower than the observed $\Delta e\text{-}m$.

Stage specificity index (Tau)

We calculated stage specificity index as:

$$\text{Tau} = \frac{\sum_{i=1}^{n}(1-\hat{x}_i)}{n-1}; \quad \hat{x}_i = \frac{x_i}{\max_{1\le i\le n}(x_i)},$$

where n is number of stages, x_i is the expression of the gene in stage i. This measure is a modified estimation of tissue specificity index of expression (Yanai et al. 2005; Kryuchkova-Mostacci and Robinson-Rechavi 2016a) and has already been applied to calculate stage specificity (Tian et al. 2013). This index ranges from zero (broadly expressed genes) to one (genes specific to one stage). All genes that were not expressed in at least one stage were removed from the analysis.

Acknowledgements

We thank Marie Zufferey and Nadezda Kryuchkova for help with preliminary work. We thank the Bgee team, Marie Zufferey, Nadezda Kryuchkova and Barbara Piasecka for help with data retrieval, Julien Roux for help with the Ensembl API, Kamil Jaron and Andrea Komljenovic for help with programing, all members of the Robinson-Rechavi lab and Hajk-Georg Drost for helpful discussions. Part of the computations were performed at the Vital-IT (http://www.vital-it.ch) centre for high-performance computing of the SIB Swiss Institute of Bioinformatics. This work was supported by Swiss National Science Foundation grant 31003A_153341 / 1.

Author contributions

JL and MRR designed the work. JL performed the data gathering and analysis. JL and MRR interpreted the results. JL wrote the first draft of the paper. JL and MRR finalized the paper.

Figures legends

Figure 1: Comparison of 95% confidence intervals from transformed and non-transformed expression values.

Dark blue, red and green marked time points in the x-axis represent early developmental stages, middle developmental stages and late developmental stages respectively. Y-axis represents the ratio of upper to lower 95% confidence interval boundary. The ratio from non-transformed expression values is plotted in dotted lines, while the ratio from $\log_2$ transformed expression values is plotted in solid lines, and the ratio from square root (abbreviated as "sqrt") transformed expression values is plotted in dashed lines.

Figure 2: Evolutionary transcriptome indexes based on $\log_2$ transformed expression values

Dark blue, red and green marked time points in the x-axis represent early developmental stages, middle developmental stages and late developmental stages respectively. Transcriptome index of divergence (TDI): blue line; transcriptome index of paralog number (TPI): pink line; transcriptome index of phyletic age (TAI): purple line. The grey area indicates 95% confidence interval estimated from bootstrap analysis. The *p*-values for supporting the hourglass model (permutation test, early *vs*. middle development) are indicated in the top-left corner of each graph.

Figure 3: Proportion of temporal pleiotropic genes across development.

Dark blue, red and green marked time points in the x-axis represent early developmental stages, middle developmental stages, and late developmental stages respectively. The proportion of temporal pleiotropic genes is plotted as orange circles. The *p*-values from chi-square goodness of fit test are indicated in the top-right corner of each graph. Pleiotropic genes are defined as expressed in more than 50% of stages sampled. The proportion of pleiotropic genes is defined as the number of pleiotropic genes divided by the number of all genes expressed in the corresponding stage.

Figure 4: Comparison of transcriptome divergence indexes (TDI) between temporal and non-temporal pleiotropic genes.

Dark blue, red and green marked time points in the x-axis represent early developmental stages, middle developmental stages and late developmental stages respectively. TDI is plotted in blue line. The grey area indicates 95% confidence interval estimated from bootstrap analysis. The *p*-values for supporting the hourglass model (permutation test, early *vs*. middle development) are indicated in the top-left corner of each graph. Upper panel graphs: temporal pleiotropic genes; lower panel graphs: non-pleiotropic genes.

Figure 5: Expression of retrogenes in development.

The median expression of retrogenes was fit by regression (the first degree of polynomial for *C. elegans* and the second degree of polynomial for other species), whose R^2 and *p*-value are indicated in the top-left corner of each graph. Dark blue, red and green marked time points in the x-axis represent early developmental stages, middle developmental stages and late developmental stages respectively. The x-axis for *C. elegans*, *D. rerio* and *D. melanogaster* is in logarithmic scale, while the x-axis for *M. musculus* is in natural scale.

Figure 6: Transcriptome index of connectivity (TCI) across development.

Dark blue, red and green marked time points in the x-axis represent early developmental stages, middle developmental stages and late developmental stages respectively. TCI is plotted in dark red line. The grey area indicates 95% confidence interval estimated from bootstrap analysis. The *p*-values for supporting the hourglass model (permutation test, early *vs*. middle development) are indicated in the top-left corner of each graph.

Figure S1: Distributions of dN and dS for *C. elegans*.

Figure S2: Evolutionary transcriptome indexes based on square root transformed expression values

Legend as Figure 2, but here the indexes are based on square root transformed expression values

Figure S3: Evolutionary transcriptome indexes based on non-transformed expression values

Legend as Figure 2, but here the indexes are based on non-transformed expression values

Figure S4: Comparison of transcriptome phyletic age indexes (TAI).

Dark blue, red and green marked time points in the x-axis represent early developmental stages, middle developmental stages and late developmental stages respectively. TAI is plotted in purple line. The grey area indicates 95% confidence interval estimated from bootstrap analysis. The *p*-values for supporting the hourglass model (permutation test, early *vs*. middle development) are indicated in the top-left corner of each graph.

A: TAI based on non-transformed expression values.

B: TAI based on $\log_2$ transformed expression values.

C: TAI based on non-transformed expression values, excluding the top 10% highly expressed genes.

Figure S5: Proportion of temporal pleiotropic genes defined as expressed in more than 70% stages.

Legend as Figure 3, but here the temporal pleiotropic genes are defined as expressed in more than 70% of stages.

Figure S6: Proportion of temporal pleiotropic genes for *C. elegans* and *D. melanogaster* after removal of the second period of late development

Legend as Figure 3.

Figure S7: Proportion of temporal pleiotropic genes for *D. rerio* based on expressed genes defined as microarray signal rank in top 90% or 50%.

Legend as Figure 3. In upper panel graphs, expressed genes defined as microarray signal rank in top 90%. In lower panel graphs, expressed genes defined as microarray signal rank in top 50%.

Figure S8: Proportion of temporal pleiotropic genes for *M. musculus* based on expressed genes defined as microarray signal rank in top 90% or 50%.

Legend as Figure 3. In upper panel graphs, expressed genes defined as microarray signal rank in top 90%. In lower panel graphs, expressed genes defined as microarray signal rank in top 50%.

Figure S9: Transcriptome index of tissue specificity (TTI) across development.

Dark blue, red and green marked time points in the x-axis represent early developmental stages, middle developmental stages and late developmental stages respectively. TTI is plotted in orange line. The grey area indicates 95% confidence interval estimated from bootstrap analysis. The *p*-values for supporting the hourglass model (permutation test, early *vs*. middle development) are indicated in the top-left corner of each graph.

Figure S10: Comparison of ω_0 between temporal pleiotropic genes and non-pleiotropic genes.

The number of genes in each category is indicated below each box. The *p*-values from a Wilcoxon test comparing categories are reported above boxes. The lower and upper intervals indicated by the dashed lines ("whiskers") represent 1.5 times the interquartile range, or the maximum (respectively minimum) if no points are beyond 1.5 IQR (default behaviour of R function boxplot).

Figure S11: Relation of protein connectivity and duplicability.

Genes were split into 10 bins according to their connectivity. The duplicability in each bin was measured by the number of genes with paralogs divided by the number of all genes. The duplicability was fit by regression (the first degree of polynomial for *C. elegans* and *M. musculus,* while the second degree of polynomial for *D. melanogaster* and *D. rerio*), whose R^2 and *p*-value are indicated in the top-left corner of each graph. The median connectivity of each bin was plotted on the x-axis (in $\log_2$ scale).

References

Abzhanov A. 2013. von Baer's law for the ages: lost and found principles of developmental evolution. Trends Genet. 29:712–722.

Artieri CG, Haerty W, Singh RS. 2009. Ontogeny and phylogeny: molecular signatures of selection, constraint, and temporal pleiotropy in the development of Drosophila. BMC Biol. 7:42.

Ballard WW. 1981. Morphogenetic Movements and Fate Maps of Vertebrates. Am. Zool. 21:391–399.

Bastian F, Parmentier G, Roux J, Moretti S, Laudet V, Robinson-Rechavi M. 2008. Bgee: Integrating and comparing heterogeneous transcriptome data among species. DILS Data Integr. Life Sci.:124–131.

Bininda-Emonds ORP, Jeffery JE, Richardson MK. 2003. Inverting the hourglass: quantitative evidence against the phylotypic stage in vertebrate development. Proc. Biol. Sci. 270:341–346.

Castillo-Davis CI, Hartl DL. 2002. Genome evolution and developmental constraint in Caenorhabditis elegans. Mol. Biol. Evol. 19:728–735.

Chen W-H, Minguez P, Lercher MJ, Bork P. 2012. OGEE: an online gene essentiality database. Nucleic Acids Res. 40:D901-6.

Cheng X, Hui JHL, Lee YY, Wan Law PT, Kwan HS. 2015. A "Developmental Hourglass" in Fungi. Mol. Biol. Evol. 32:1556–1566.

Comte A, Roux J, Robinson-Rechavi M. 2010. Molecular signaling in zebrafish development and the vertebrate phylotypic period. Evol. Dev. 12:144–156.

Cruickshank T, Wade MJ. 2008. Microevolutionary support for a developmental hourglass: gene expression patterns shape sequence variation and divergence in *Drosophila*. Evol. Dev. 10:583–590.

Cutter AD, Ward S. 2005. Sexual and Temporal Dynamics of Molecular Evolution in C. elegans Development. Mol. Biol. Evol. 22:178–188.

Davis JC, Brandman O, Petrov DA. 2005. Protein evolution in the context of Drosophila development. J. Mol. Evol. 60:774–785.

Domazet-Loso T, Tautz D. 2010. A phylogenetically based transcriptome age index mirrors ontogenetic divergence patterns. Nature 468:815–818.

Drost H-G, Gabel A, Domazet-Lošo T, Quint M, Grosse I. 2016. Capturing Evolutionary Signatures in Transcriptomes with myTAI. bioRxiv:doi:10.1101/051565.

Drost H-G, Gabel A, Grosse I, Quint M. 2015. Evidence for active maintenance of phylotranscriptomic hourglass patterns in animal and plant embryogenesis. Mol. Biol. Evol. 32:1221–1231.

Duboule D. 1994. Temporal colinearity and the phylotypic progression: a basis for the stability of a vertebrate Bauplan and the evolution of morphologies through heterochrony. Development 1994:135–142.

Dunn CW, Zapata F, Munro C, Siebert S, Hejnol A. 2018. Pairwise comparisons across species are problematic when analyzing functional genomic data. Proc. Natl. Acad. Sci. U. S. A.:201707515.

Fraser HB, Hirsh AE, Steinmetz LM, Scharfe C, Feldman MW. 2002. Evolutionary Rate in the Protein Interaction Network. Science (80-.). 296:750–752.

Fu B, Chen M, Zou M, Long M, He S. 2010. The rapid generation of chimerical genes expanding protein diversity in zebrafish. BMC Genomics 11:657.

Galis F, Metz JA. 2001. Testing the vulnerability of the phylotypic stage: on modularity and evolutionary conservation. J. Exp. Zool. 291:195–204.

Garstang W. 1922. The Theory of Recapitulation: A Critical Re-statement of the Biogenetic Law. J. Linn. Soc. London, Zool. 35:81–101.
Gerstein MB, Lu ZJ, Van Nostrand EL, Cheng C, Arshinoff BI, Liu T, Yip KY, Robilotto R, Rechtsteiner A, Ikegami K, et al. 2010. Integrative Analysis of the Caenorhabditis elegans Genome by the modENCODE Project. Science (80-.). 330:1775–1787.
Gerstein MB, Rozowsky J, Yan K-K, Wang D, Cheng C, Brown JB, Davis CA, Hillier L, Sisu C, Li JJ, et al. 2014. Comparative analysis of the transcriptome across distant species. Nature 512:445–448.
Graveley BR, Brooks AN, Carlson JW, Duff MO, Landolin JM, Yang L, Artieri CG, van Baren MJ, Boley N, Booth BW, et al. 2011. The developmental transcriptome of Drosophila melanogaster. Nature 471:473–479.
Hanada K, Shiu S-H, Li W-H. 2007. The nonsynonymous/synonymous substitution rate ratio versus the radical/conservative replacement rate ratio in the evolution of mammalian genes. Mol. Biol. Evol. 24:2235–2241.
Hazkani-Covo E, Wool D, Graur D. 2005. In search of the vertebrate phylotypic stage: a molecular examination of the developmental hourglass model and von Baer's third law. J. Exp. Zool. B. Mol. Dev. Evol. 304:150–158.
Hu H, Uesaka M, Guo S, Shimai K, Lu T-M, Li F, Fujimoto S, Ishikawa M, Liu S, Sasagawa Y, et al. 2017. Constrained vertebrate evolution by pleiotropic genes. Nat. Ecol. Evol. 1:1722–1730.
Hughes AL, Friedman R. 2005. Gene Duplication and the Properties of Biological Networks. J. Mol. Evol. 61:758–764.
Irie N, Kuratani S. 2011. Comparative transcriptome analysis reveals vertebrate phylotypic period during organogenesis. Nat. Commun. 2:248.
Irie N, Kuratani S. 2014. The developmental hourglass model: a predictor of the basic body plan? Development 141:4649–4655.
Irie N, Sehara-Fujisawa A. 2007. The vertebrate phylotypic stage and an early bilaterian-related stage in mouse embryogenesis defined by genomic information. BMC Biol. 5:1.
Kabza M, Ciomborowska J, Maka owska I. 2014. RetrogeneDB--A Database of Animal Retrogenes. Mol. Biol. Evol. 31:1646–1648.
Kaessmann H. 2010. Origins, evolution, and phenotypic impact of new genes. Genome Res. 20:1313–1326.
Kaessmann H, Vinckenbosch N, Long M. 2009. RNA-based gene duplication: mechanistic and evolutionary insights. Nat. Rev. Genet. 10:19–31.
Kalinka AT, Tomancak P. 2012. The evolution of early animal embryos: conservation or divergence? Trends Ecol. Evol. 27:385–393.
Kalinka AT, Varga KM, Gerrard DT, Preibisch S, Corcoran DL, Jarrells J, Ohler U, Bergman CM, Tomancak P. 2010. Gene expression divergence recapitulates the developmental hourglass model. Nature 468:811–814.
Kersey PJ, Allen JE, Armean I, Boddu S, Bolt BJ, Carvalho-Silva D, Christensen M, Davis P, Falin LJ, Grabmueller C, et al. 2016. Ensembl Genomes 2016: more genomes, more complexity. Nucleic Acids Res. 44:D574–D580.
Kinsella RJ, Kahari A, Haider S, Zamora J, Proctor G, Spudich G, Almeida-King J, Staines D, Derwent P, Kerhornou A, et al. 2011. Ensembl BioMarts: a hub for data retrieval across taxonomic space. Database 2011:bar030.
Kryuchkova-Mostacci N, Robinson-Rechavi M. 2015. Tissue-Specific Evolution of Protein Coding Genes in Human and Mouse. PLoS One 10:1–15.
Kryuchkova-Mostacci N, Robinson-Rechavi M. 2016a. A benchmark of gene

expression tissue-specificity metrics. Brief. Bioinform. 18:205–214.
Kryuchkova-Mostacci N, Robinson-Rechavi M. 2016b. Tissue-Specificity of Gene Expression Diverges Slowly between Orthologs, and Rapidly between Paralogs.Ouzounis CA, editor. PLOS Comput. Biol. 12:e1005274.
Larracuente AM, Sackton TB, Greenberg AJ, Wong A, Singh ND, Sturgill D, Zhang Y, Oliver B, Clark AG, Zuckerkandl E, et al. 2008. Evolution of protein-coding genes in Drosophila. Trends Genet. 24:114–123.
Levin M, Anavy L, Cole AG, Winter E, Mostov N, Khair S, Senderovich N, Kovalev E, Silver DH, Feder M, et al. 2016. The mid-developmental transition and the evolution of animal body plans. Nature 531:637–641.
Levin M, Hashimshony T, Wagner F, Yanai I, Arbeitman MN, Furlong EE, Imam F, Johnson E, Null BH, Baker BS, et al. 2012. Developmental milestones punctuate gene expression in the Caenorhabditis embryo. Dev. Cell 22:1101–1108.
Li JJ, Huang H, Bickel PJ, Brenner SE. 2014. Comparison of D. melanogaster and C. elegans developmental stages, tissues, and cells by modENCODE RNA-seq data. Genome Res. 24:1086–1101.
Liu J, Robinson-Rechavi M. 2017. Adaptive evolution of proteins expressed in late and post-embryonic development in animals. bioRxiv:doi:10.1101/161711.
Moretti S, Laurenczy B, Gharib WH, Castella B, Kuzniar A, Schabauer H, Studer R a., Valle M, Salamin N, Stockinger H, et al. 2014. Selectome update: Quality control and computational improvements to a database of positive selection. Nucleic Acids Res. 42:917–921.
Ninova M, Ronshaugen M, Griffiths-Jones S. 2014. Conserved temporal patterns of microRNA expression in Drosophila support a developmental hourglass model. Genome Biol. Evol. 6:2459–2467.
Papp B, Pál C, Hurst LD. 2003. Dosage sensitivity and the evolution of gene families in yeast. Nature 424:194–197.
Piasecka B, Lichocki P, Moretti S, Bergmann S, Robinson-Rechavi M. 2013. The Hourglass and the Early Conservation Models—Co-Existing Patterns of Developmental Constraints in Vertebrates.Barsh GS, editor. PLoS Genet. 9:e1003476.
Poe S, Wake MH. 2004. Quantitative tests of general models for the evolution of development. Am. Nat. 164:415–422.
Prachumwat A, Li W-H. 2006. Protein function, connectivity, and duplicability in yeast. Mol. Biol. Evol. 23:30–39.
Quint M, Drost H-G, Gabel A, Ullrich KK, Bönn M, Grosse I. 2012. A transcriptomic hourglass in plant embryogenesis. Nature 490:98–101.
Raff RA. 1996. The shape of life : genes, development, and the evolution of animal form. University of Chicago Press.
Richardson MK. 1995. Heterochrony and the phylotypic period. Dev. Biol. 172:412–421.
Richardson MK, Hanken J, Gooneratne ML, Pieau C, Raynaud A, Selwood L, Wright GM. 1997. There is no highly conserved embryonic stage in the vertebrates: implications for current theories of evolution and development. Anat. Embryol. (Berl). 196:91–106.
Riedl R. 1978. Order in living organisms. West Sussex, UK: Wiley-Interscience.
Roux J, Robinson-Rechavi M. 2008. Developmental constraints on vertebrate genome evolution. PLoS Genet. 4:e1000311.
Sander K. 1983. Development and evolution: the sixth Symposium of the British Society for Developmental Biology. Cambridge University Press.

Slack JMW, Holland PWH, Graham CF. 1993. The zootype and the phylotypic stage. Nature 361:490–492.
Soumillon M, Necsulea A, Weier M, Brawand D, Zhang X, Gu H, Barthès P, Kokkinaki M, Nef S, Gnirke A, et al. 2013. Cellular Source and Mechanisms of High Transcriptome Complexity in the Mammalian Testis. Cell Rep. 3:2179–2190.
Tadros W, Lipshitz HD. 2009. The maternal-to-zygotic transition: a play in two acts. Development 136:3033–3042.
Tian X, Strassmann JE, Queller DC. 2013. Dictyostelium Development Shows a Novel Pattern of Evolutionary Conservation. Mol. Biol. Evol. 30:977–984.
Veitia RA. 2002. Exploring the etiology of haploinsufficiency. BioEssays 24:175–184.
Von-Baer KE. 1828. Über Entwickelungsgeschichte der Tiere: Beobachtung und Reflexion. Königsberg: Gebrüder Bornträger.
Wagner GP, Zhang J. 2011. The pleiotropic structure of the genotype–phenotype map: the evolvability of complex organisms. Nat. Rev. Genet. 12:204–213.
Wang Z, Pascual-Anaya J, Zadissa A, Li W, Niimura Y, Huang Z, Li C, White S, Xiong Z, Fang D, et al. 2013. The draft genomes of soft-shell turtle and green sea turtle yield insights into the development and evolution of the turtle-specific body plan. Nat. Genet. 45:701–706.
Wolpert L. 1991. The Triumph of the Embryo. Oxford University Press.
Yanai I, Benjamin H, Shmoish M, Chalifa-Caspi V, Shklar M, Ophir R, Bar-Even A, Horn-Saban S, Safran M, Domany E, et al. 2005. Genome-wide midrange transcription profiles reveal expression level relationships in human tissue specification. Bioinformatics 21:650–659.
Yanai I, Peshkin L, Jorgensen P, Kirschner MW. 2011. Mapping gene expression in two Xenopus species: evolutionary constraints and developmental flexibility. Dev. Cell 20:483–496.
Yates A, Akanni W, Amode MR, Barrell D, Billis K, Carvalho-Silva D, Cummins C, Clapham P, Fitzgerald S, Gil L, et al. 2016. Ensembl 2016. Nucleic Acids Res. 44:D710–D716.
Zalts H, Yanai I, Huber W, Salzberg SL, Hunter CP. 2017. Developmental constraints shape the evolution of the nematode mid-developmental transition. Nat. Ecol. Evol. 1:113.
Zhang J, Nielsen R, Yang Z. 2005. Evaluation of an improved branch-site likelihood method for detecting positive selection at the molecular level. Mol. Biol. Evol. 22:2472–2479.
Zou M, Wang G, He S. 2012. Evolutionary patterns of RNA-based gene duplicates in Caenorhabditis nematodes coincide with their genomic features. BMC Res. Notes 5:398.

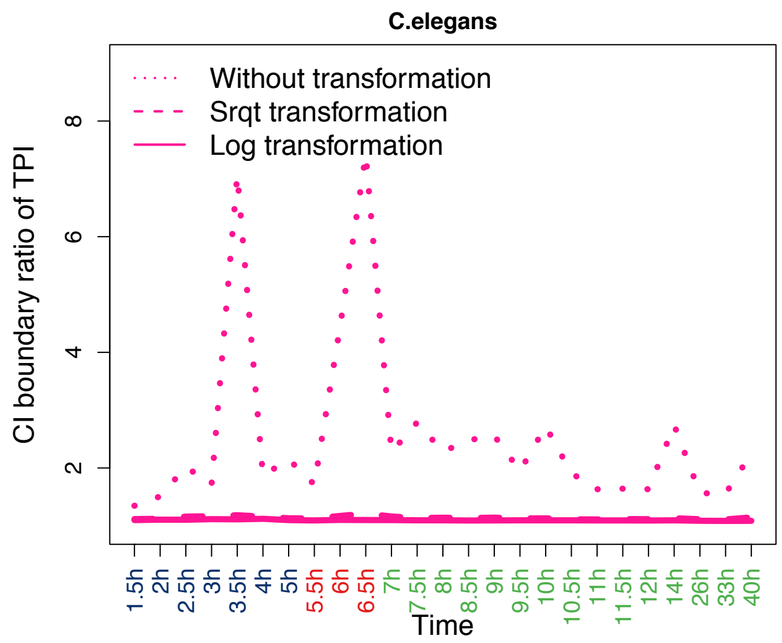
C.elegans
Without transformation
Srqt transformation
Log transformation
CI boundary ratio of TPI
Time

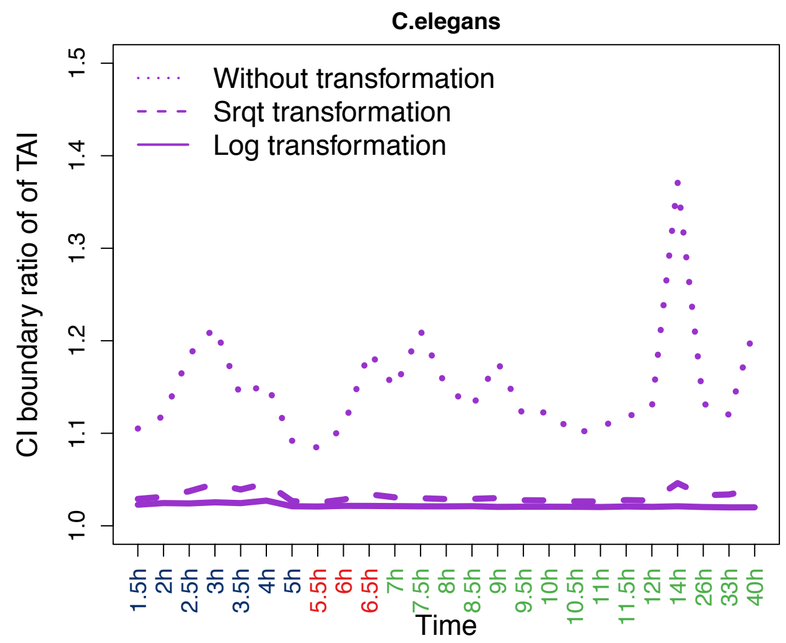
C.elegans
Without transformation
Srqt transformation
Log transformation
CI boundary ratio of of TAI
Time

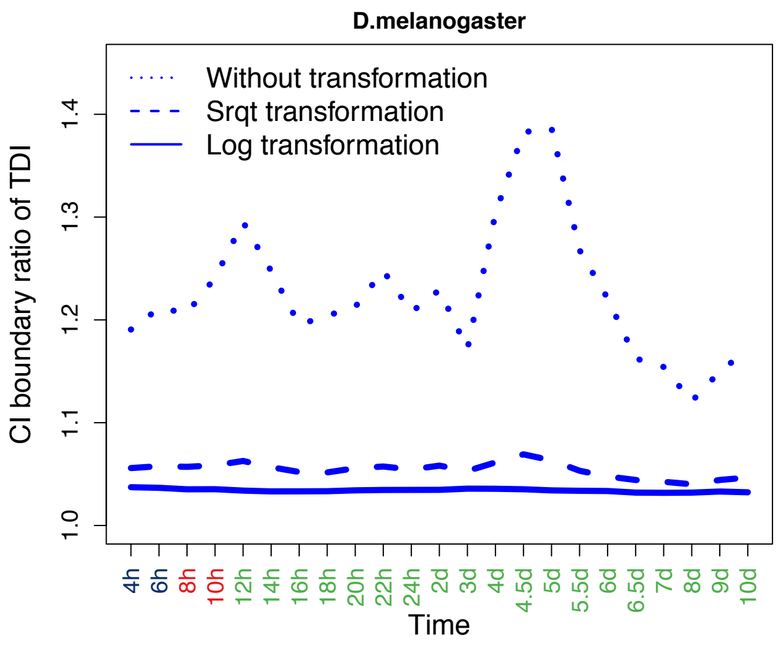
D.melanogaster
Without transformation
Srqt transformation
Log transformation
CI boundary ratio of TDI
Time

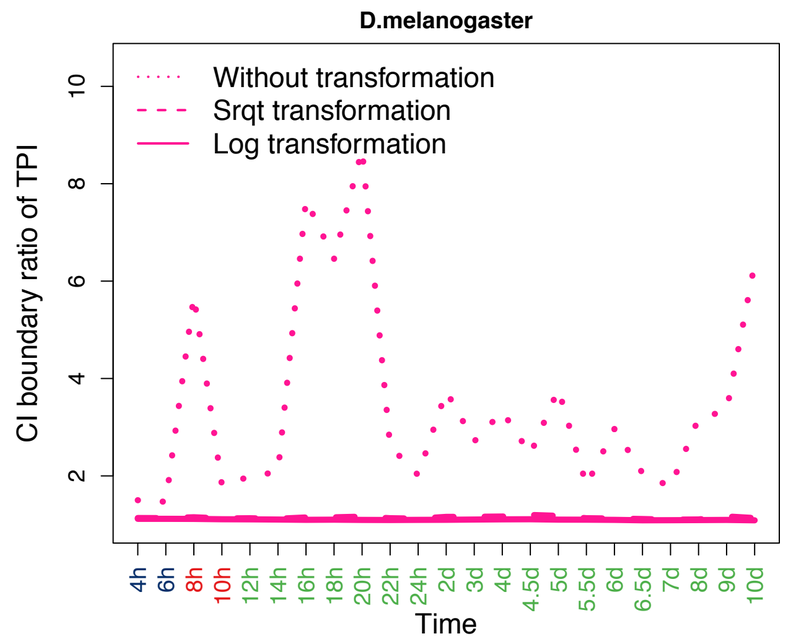
D.melanogaster
Without transformation
Srqt transformation
Log transformation
CI boundary ratio of TPI
Time

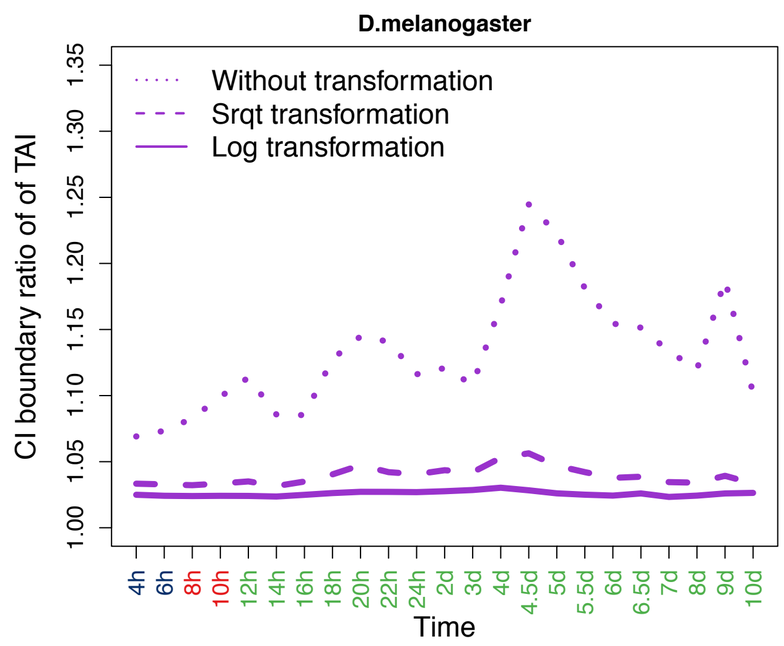
D.melanogaster
Without transformation
Srqt transformation
Log transformation
CI boundary ratio of of TAI
Time

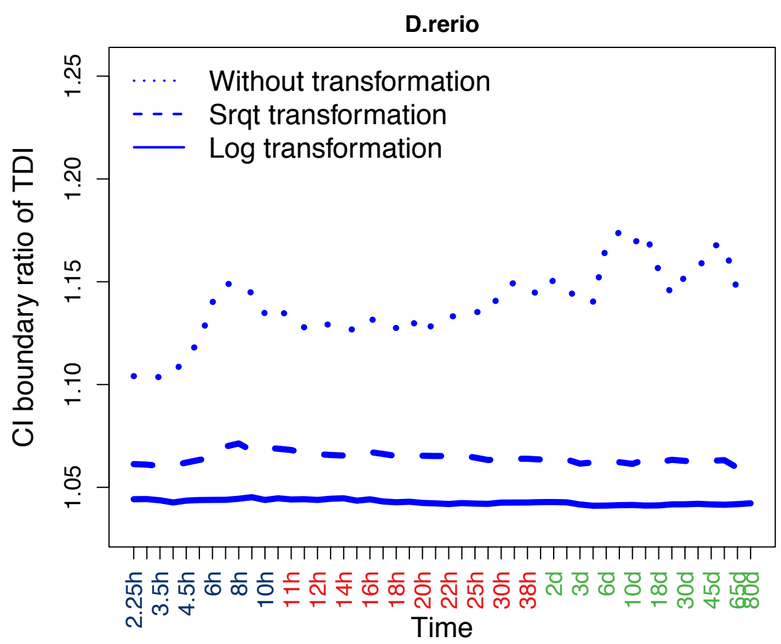
D.rerio
Without transformation
Srqt transformation
Log transformation
CI boundary ratio of TDI
Time

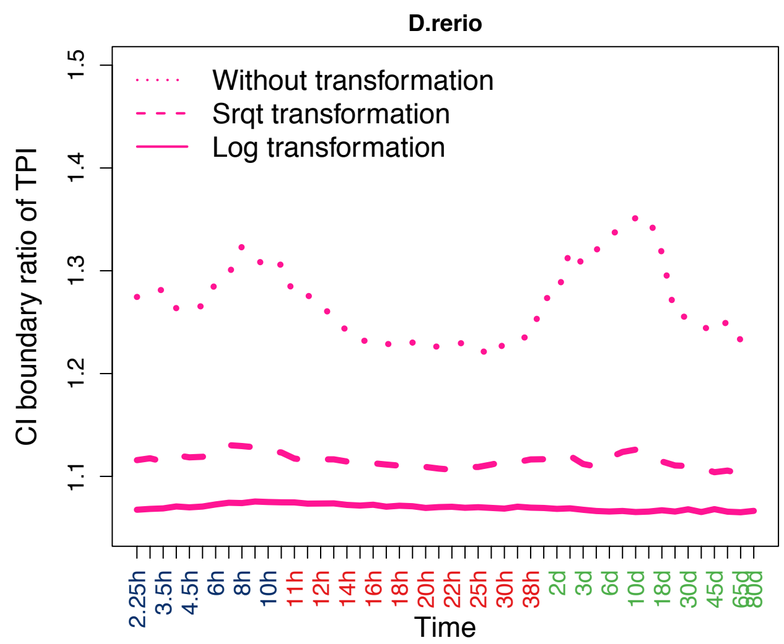
D.rerio
Without transformation
Srqt transformation
Log transformation
CI boundary ratio of TPI
Time

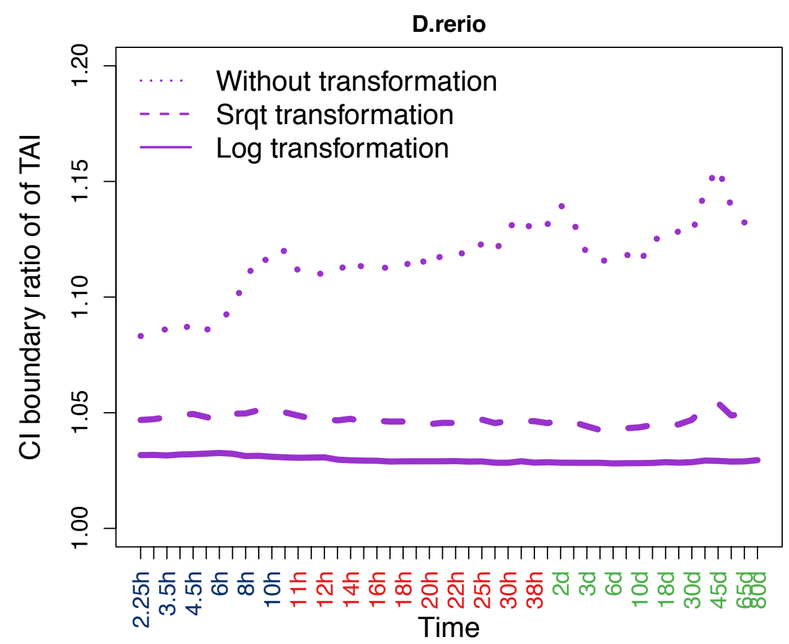
D.rerio
Without transformation
Srqt transformation
Log transformation
CI boundary ratio of of TAI
Time

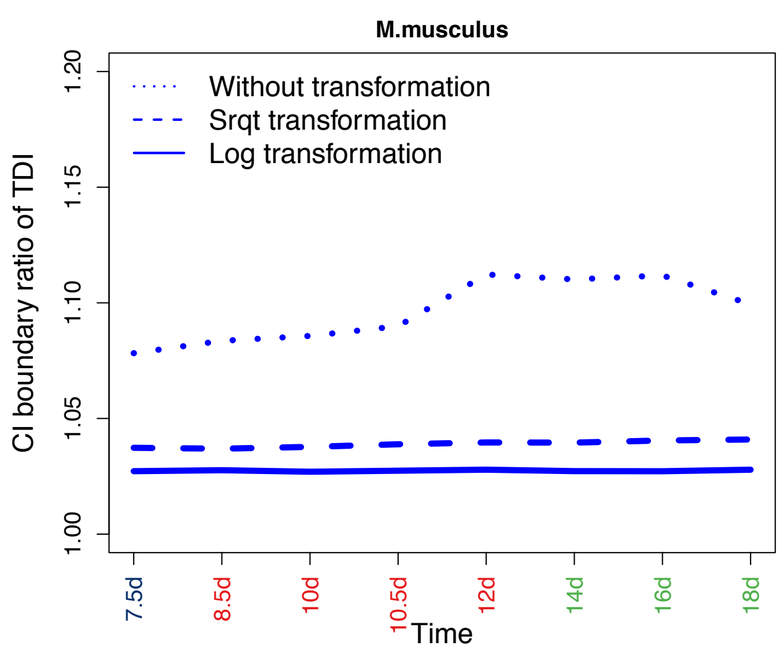
M.musculus
Without transformation
Srqt transformation
Log transformation
CI boundary ratio of TDI
Time

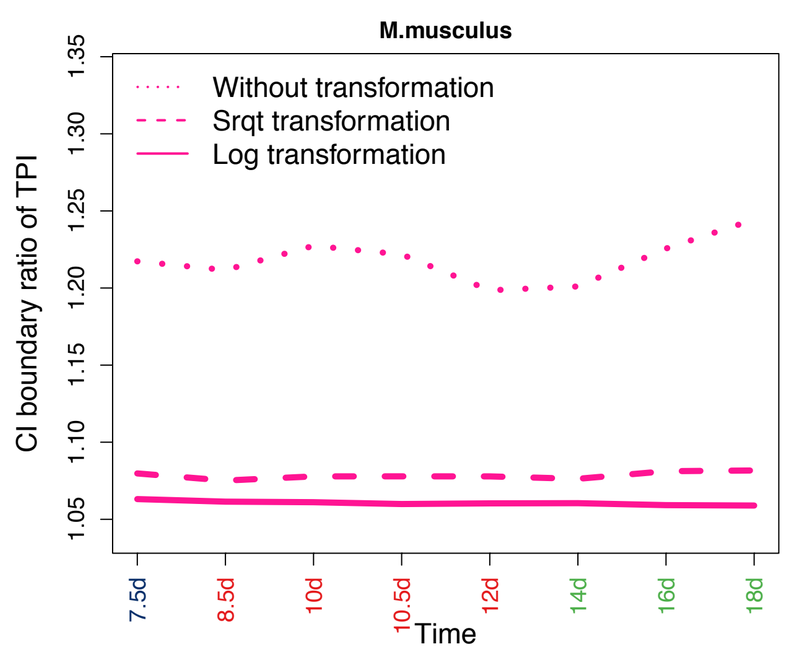
M.musculus
Without transformation
Srqt transformation
Log transformation
CI boundary ratio of TPI
Time

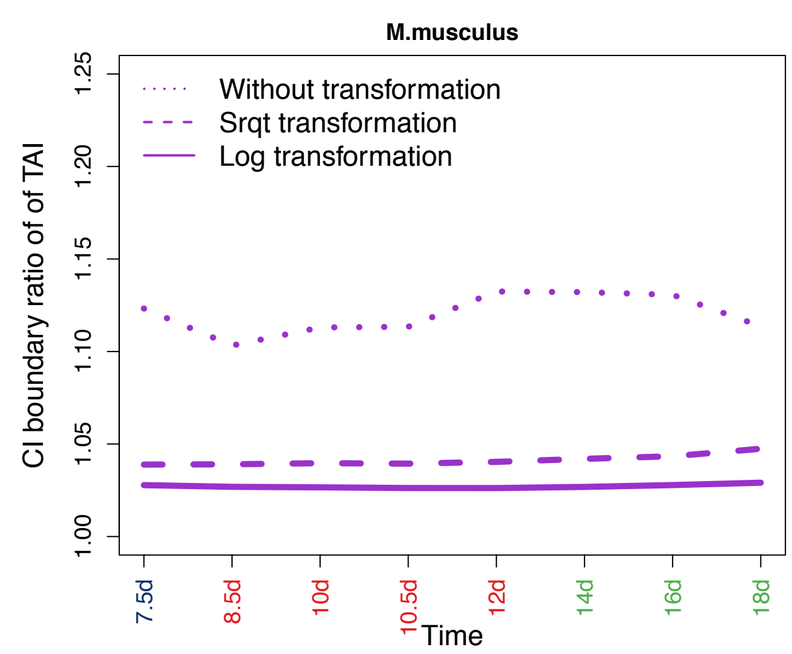
M.musculus
Without transformation
Srqt transformation
Log transformation
CI boundary ratio of of TAI
Time

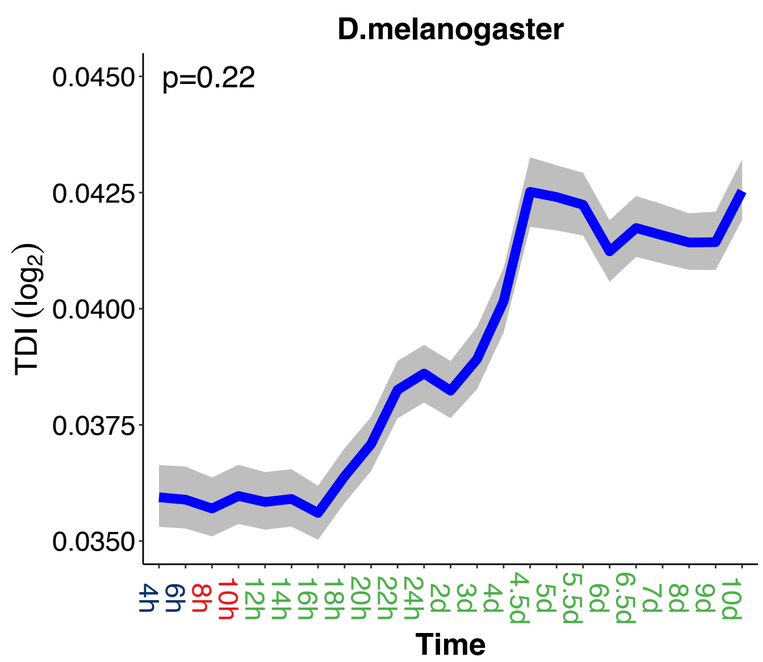
D.melanogaster
p=0.22
TDI (log2)
0.0450
0.0425
0.0400
0.0375
0.0350
4h 6h 8h 10h 12h 14h 16h 18h 20h 22h 24h 2d 3d 4d 4.5d 5d 5.5d 6d 6.5d 7d 8d 9d 10d
Time

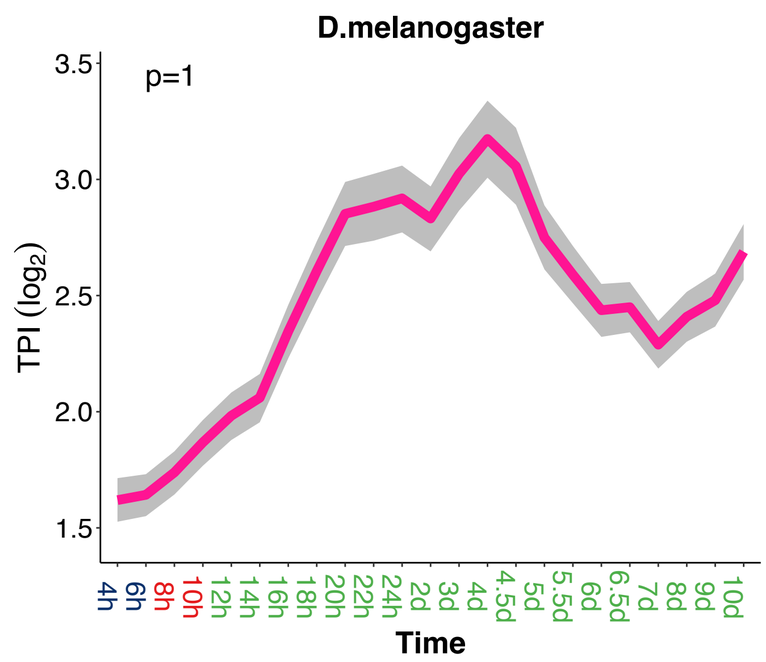
D.melanogaster
p=1
TPI (log2)
3.5
3.0
2.5
2.0
1.5
4h 6h 8h 10h 12h 14h 16h 18h 20h 22h 24h 2d 3d 4d 4.5d 5d 5.5d 6d 6.5d 7d 8d 9d 10d
Time

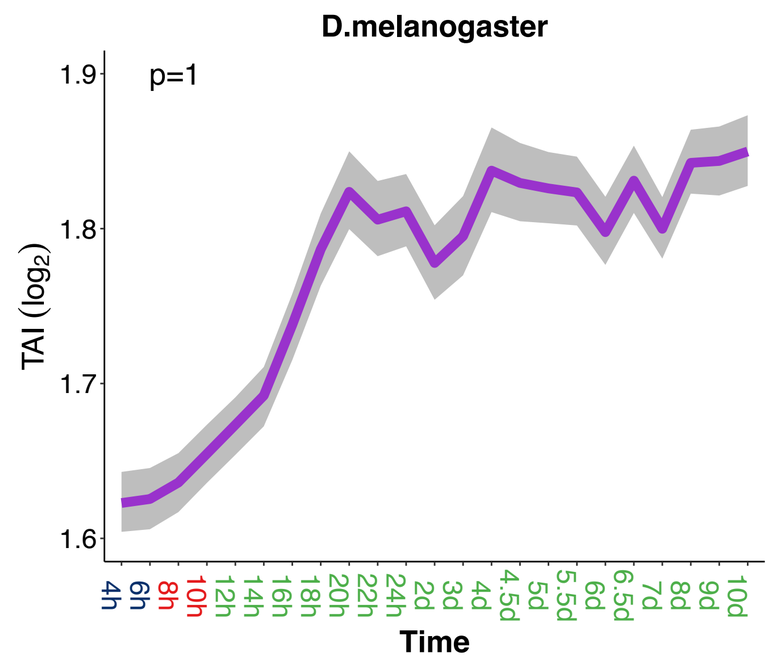
D.melanogaster
p=1
TAI (log2)
1.9
1.8
1.7
1.6
4h 6h 8h 10h 12h 14h 16h 18h 20h 22h 24h 2d 3d 4d 4.5d 5d 5.5d 6d 6.5d 7d 8d 9d 10d
Time

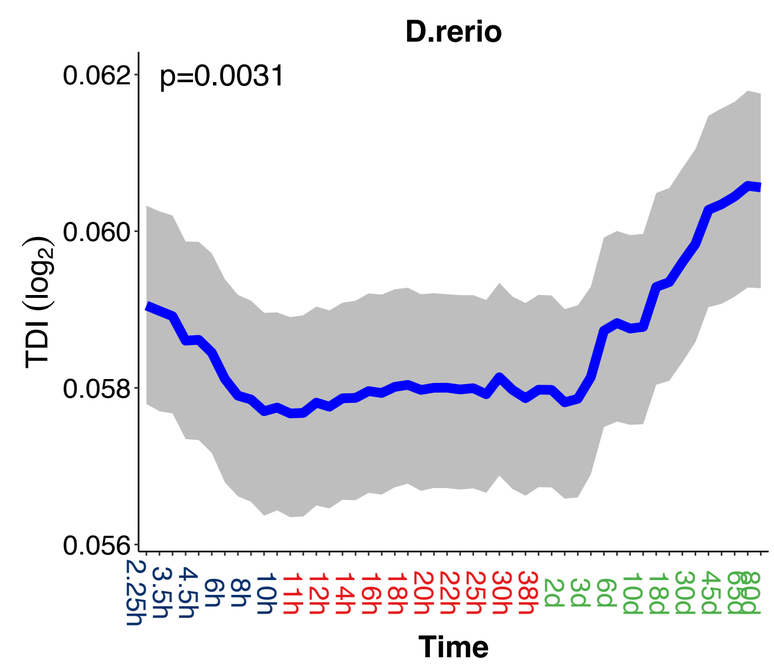
D.rerio
p=0.0031
TDI (log2)
0.062
0.060
0.058
0.056
2.25h 3.5h 4.5h 6h 8h 10h 11h 12h 14h 16h 18h 20h 22h 25h 30h 38h 2d 3d 6d 10d 18d 30d 45d 60d 80d
Time

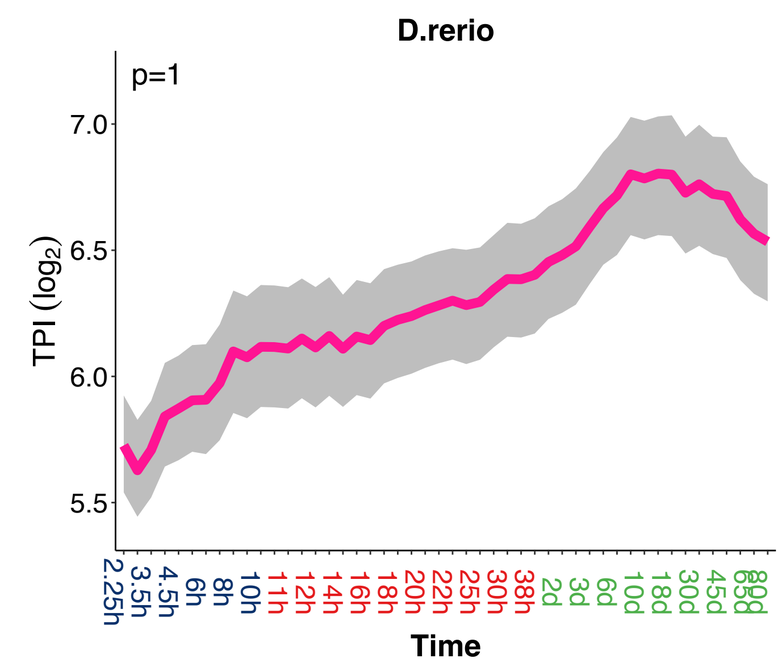
D.rerio
p=1
TPI (log2)
7.0
6.5
6.0
5.5
2.25h 3.5h 4.5h 6h 8h 10h 11h 12h 14h 16h 18h 20h 22h 25h 30h 38h 2d 3d 6d 10d 18d 30d 45d 60d 80d
Time

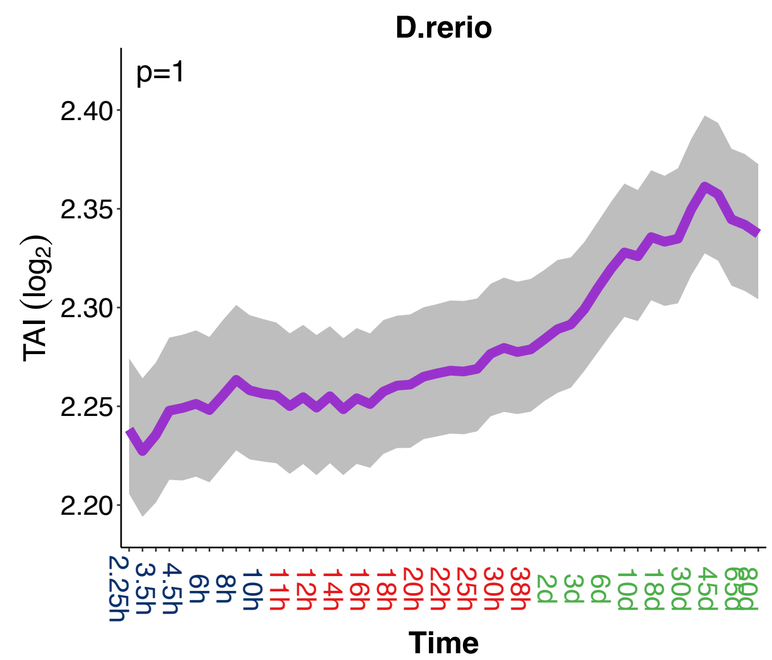
D.rerio
p=1
TAI (log2)
2.40
2.35
2.30
2.25
2.20
2.25h 3.5h 4.5h 6h 8h 10h 11h 12h 14h 16h 18h 20h 22h 25h 30h 38h 2d 3d 6d 10d 18d 30d 45d 60d 80d
Time

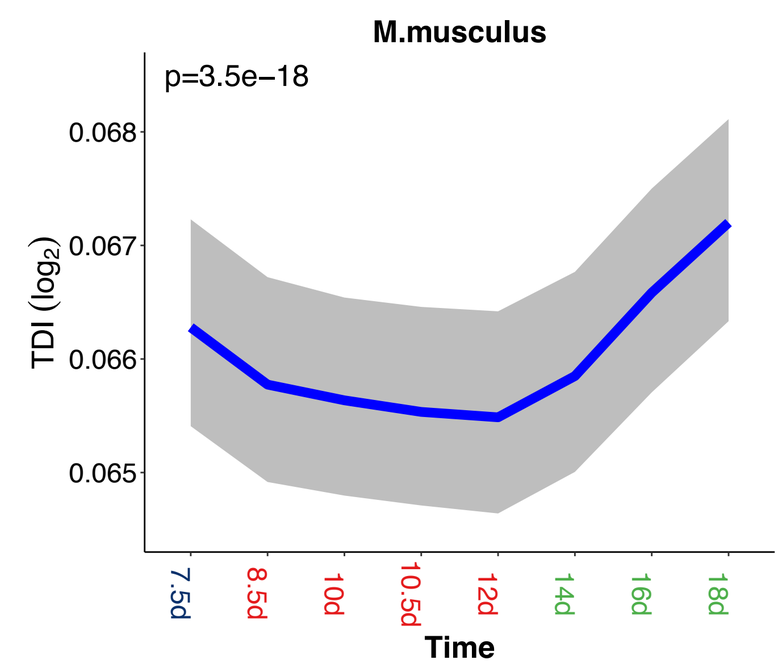
M.musculus
p=3.5e−18
TDI (log2)
0.068
0.067
0.066
0.065
7.5d 8.5d 10d 10.5d 12d 14d 16d 18d
Time

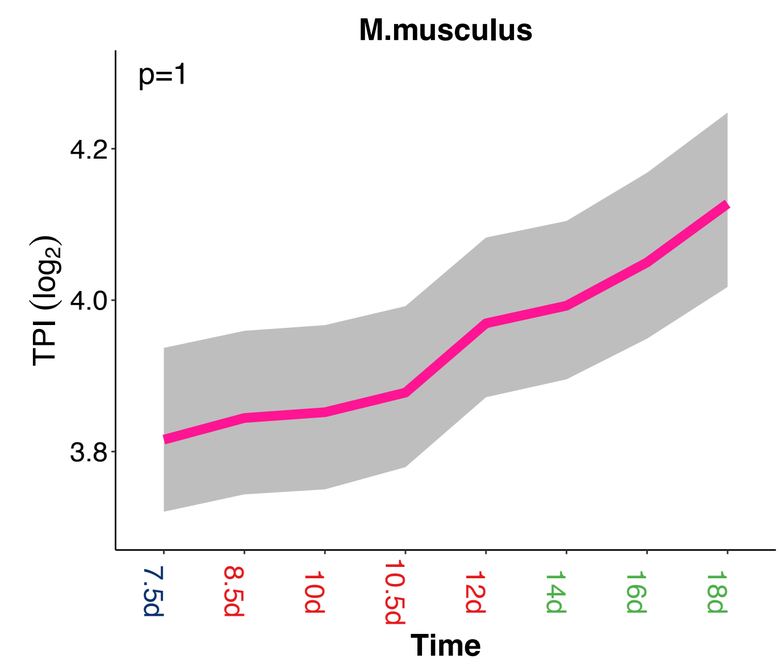
M.musculus
p=1
TPI (log2)
4.2
4.0
3.8
7.5d 8.5d 10d 10.5d 12d 14d 16d 18d
Time

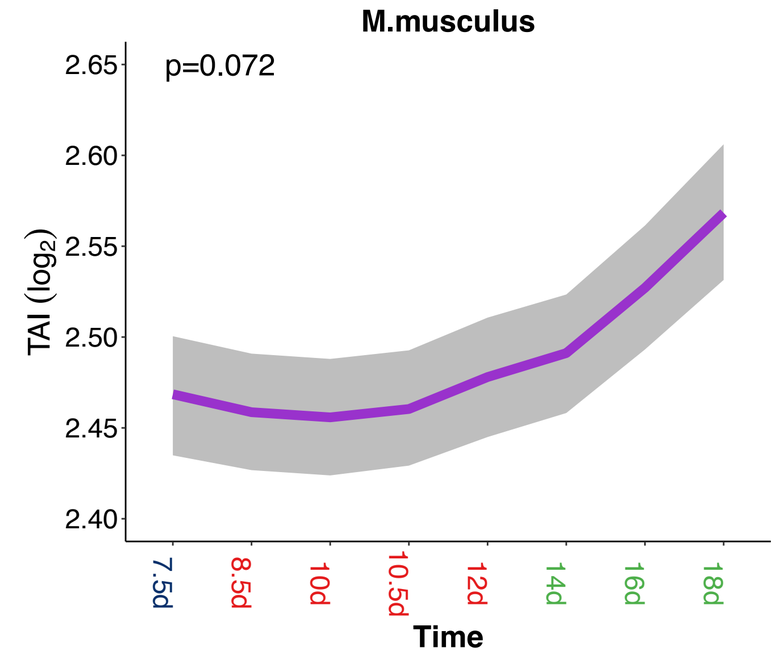
M.musculus
p=0.072
TAI (log2)
2.65
2.60
2.55
2.50
2.45
2.40
7.5d 8.5d 10d 10.5d 12d 14d 16d 18d
Time

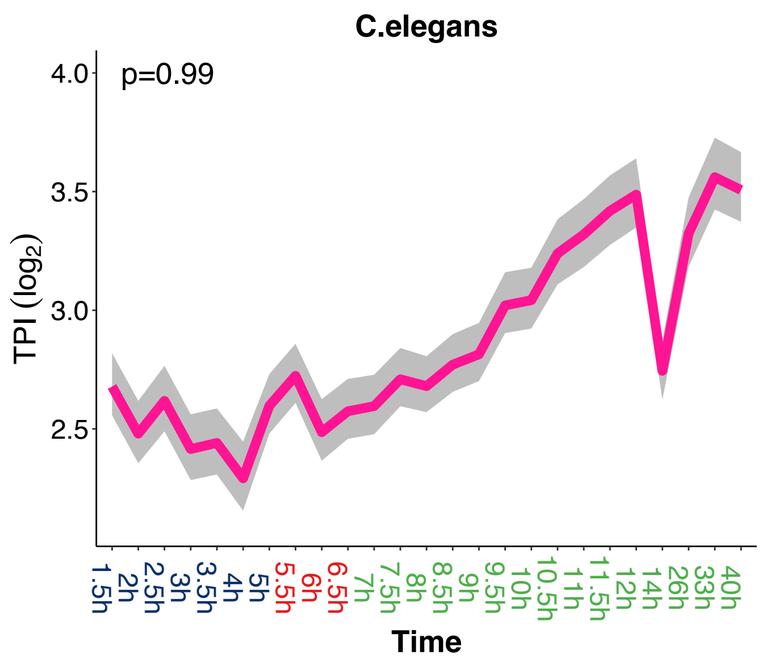
C.elegans
p=0.99
TPI (log2)
4.0
3.5
3.0
2.5
1.5h 2h 2.5h 3h 3.5h 4h 5h 5.5h 6h 6.5h 7h 7.5h 8h 8.5h 9h 9.5h 10h 10.5h 11h 11.5h 12h 14h 26h 33h 40h
Time

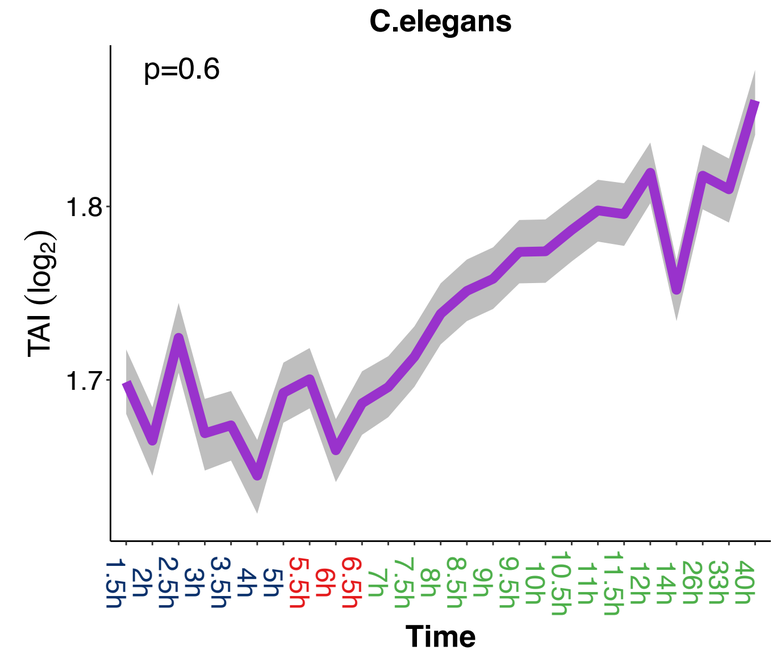
C.elegans
p=0.6
TAI (log2)
1.8
1.7
1.5h 2h 2.5h 3h 3.5h 4h 5h 5.5h 6h 6.5h 7h 7.5h 8h 8.5h 9h 9.5h 10h 10.5h 11h 11.5h 12h 14h 26h 33h 40h
Time

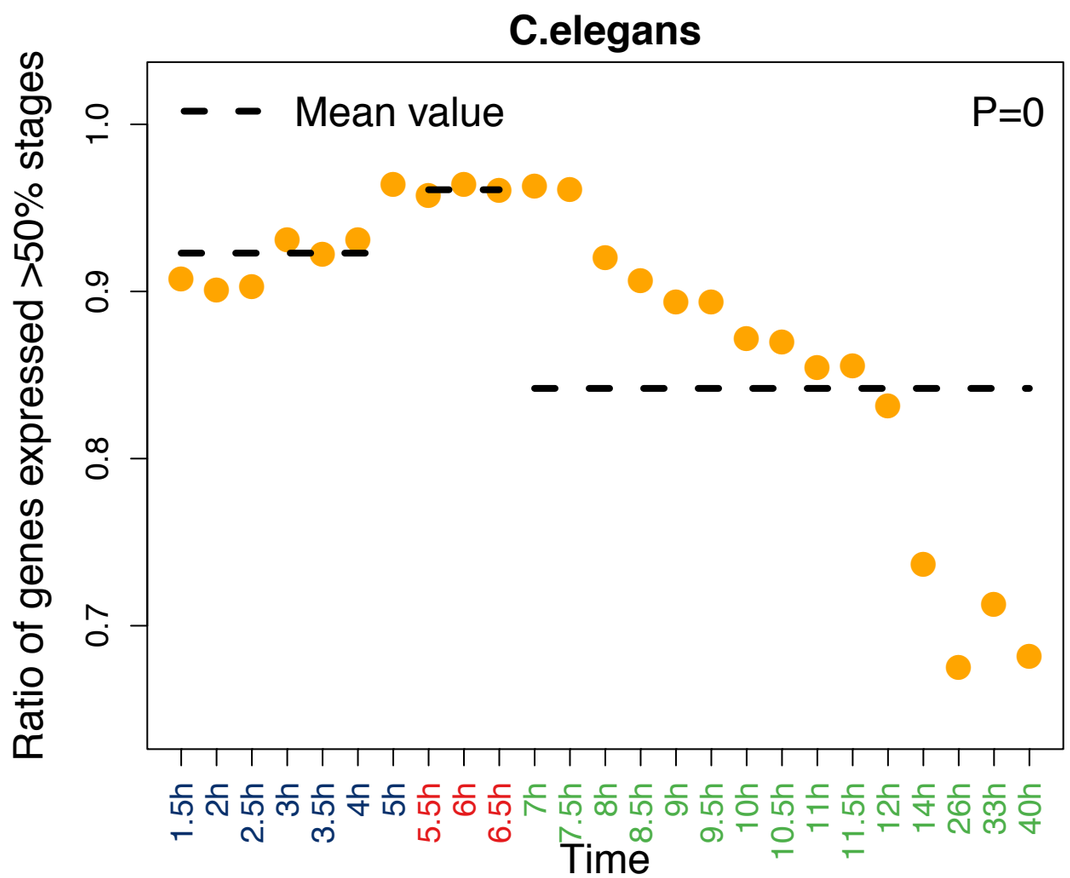
C.elegans
Mean value
P=0
Ratio of genes expressed >50% stages
1.0
0.9
0.8
0.7
1.5h
2h
2.5h
3h
3.5h
4h
5h
5.5h
6h
6.5h
7h
7.5h
8h
8.5h
9h
9.5h
10h
10.5h
11h
11.5h
12h
14h
26h
33h
40h
Time

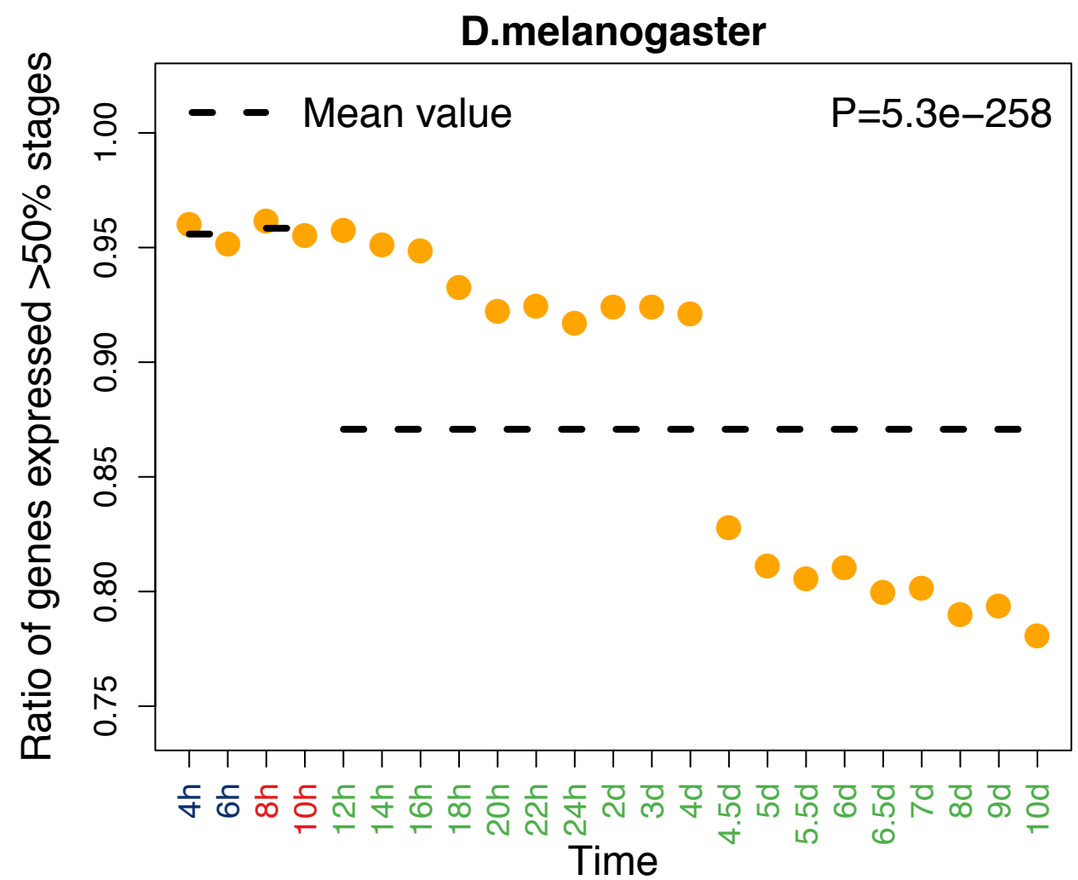
D.melanogaster
Mean value
P=5.3e−258
Ratio of genes expressed >50% stages
1.00
0.95
0.90
0.85
0.80
0.75
4h
6h
8h
10h
12h
14h
16h
18h
20h
22h
24h
2d
3d
4d
4.5d
5d
5.5d
6d
6.5d
7d
8d
9d
10d
Time

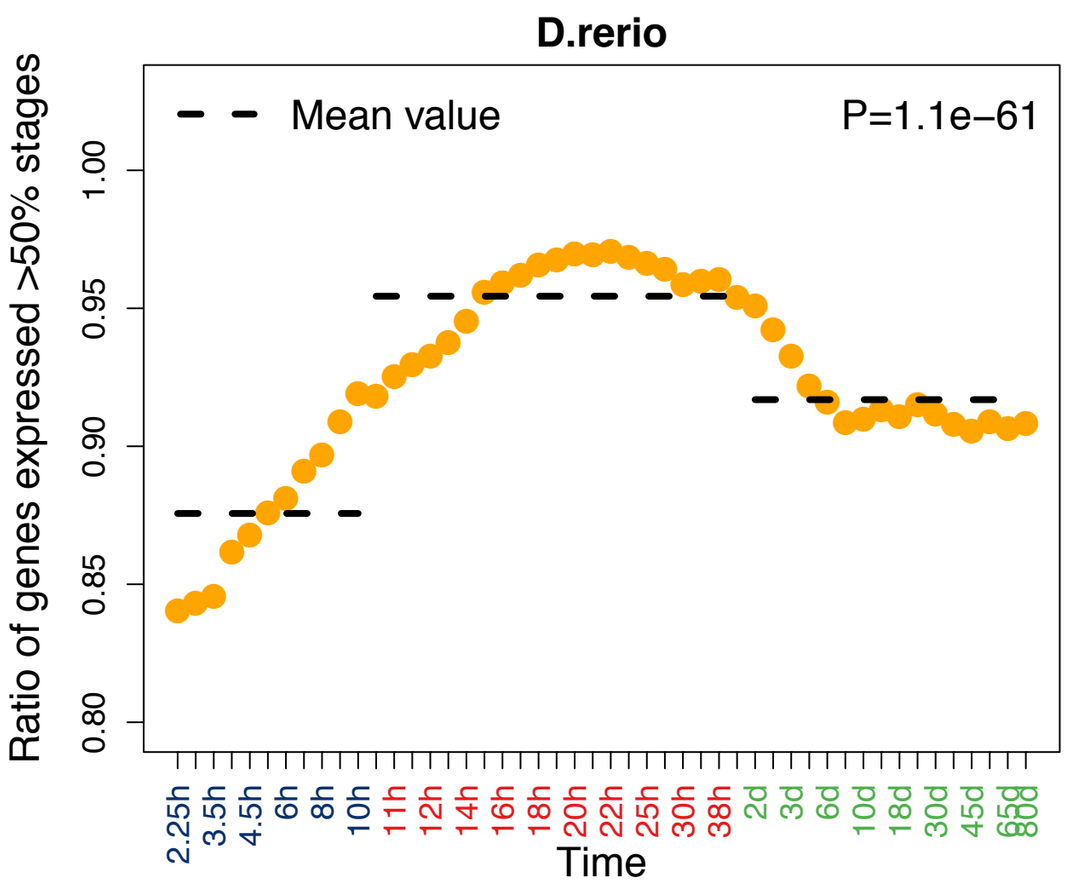
D.rerio
Mean value
P=1.1e−61
Ratio of genes expressed >50% stages
1.00
0.95
0.90
0.85
0.80
2.25h
3.5h
4.5h
6h
8h
10h
11h
12h
14h
16h
18h
20h
22h
25h
30h
38h
2d
3d
6d
10d
18d
30d
45d
65d
80d
Time

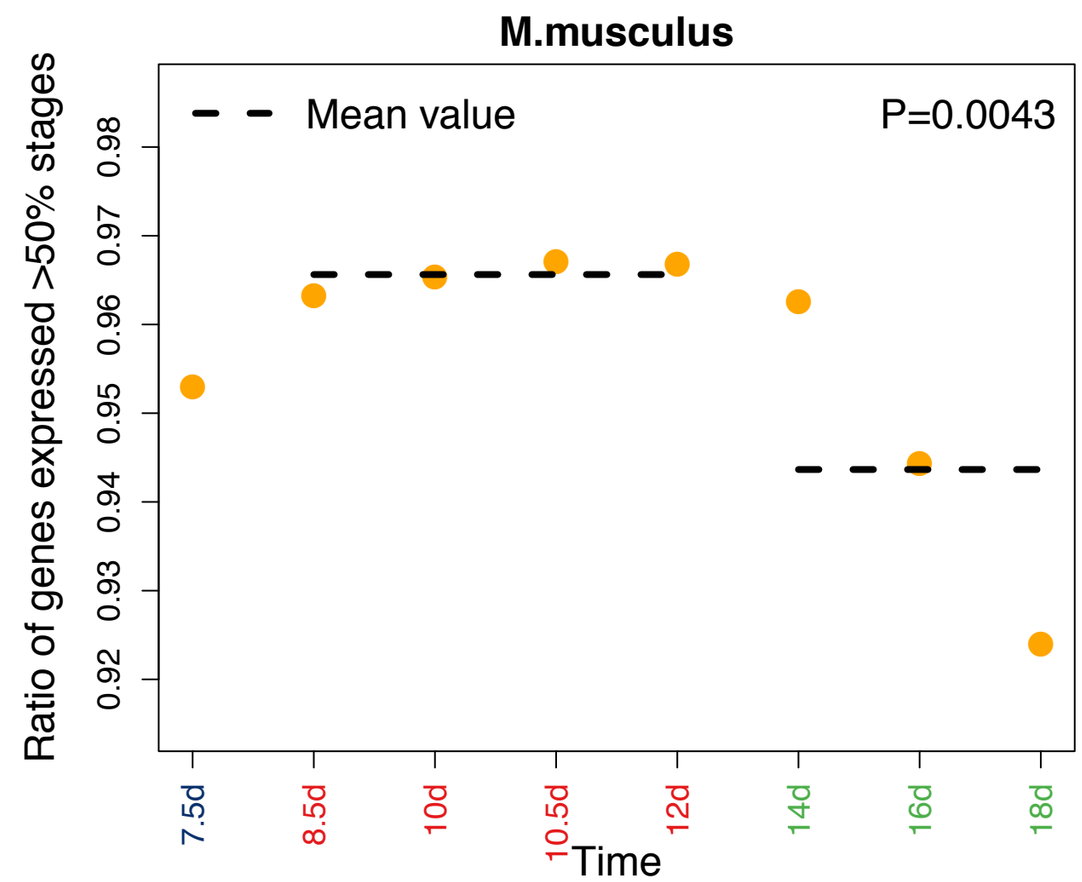
M.musculus
Mean value
P=0.0043
Ratio of genes expressed >50% stages
0.98
0.97
0.96
0.95
0.94
0.93
0.92
7.5d
8.5d
10d
10.5d
12d
14d
16d
18d
Time

Pleiotropic genes

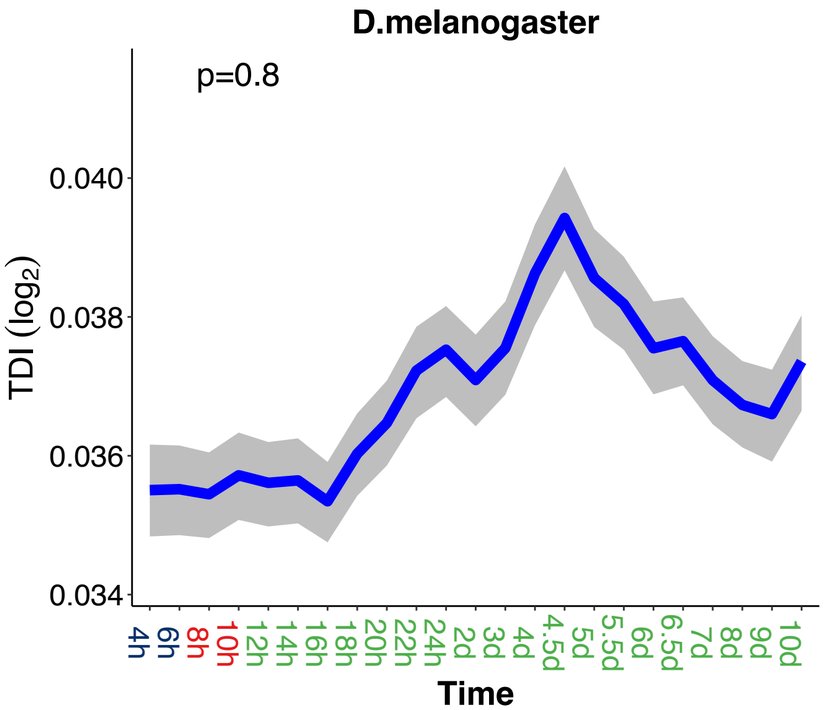

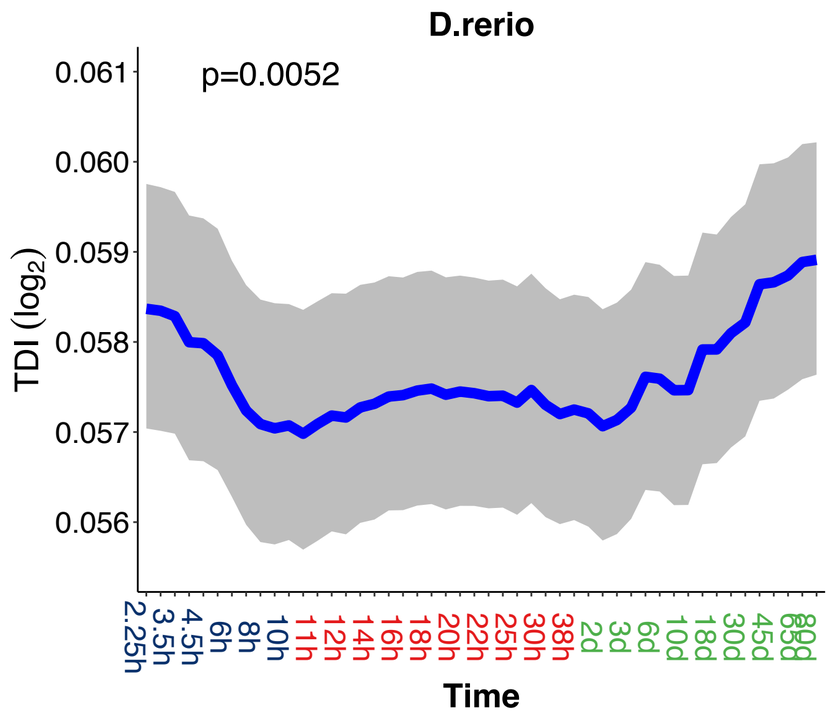

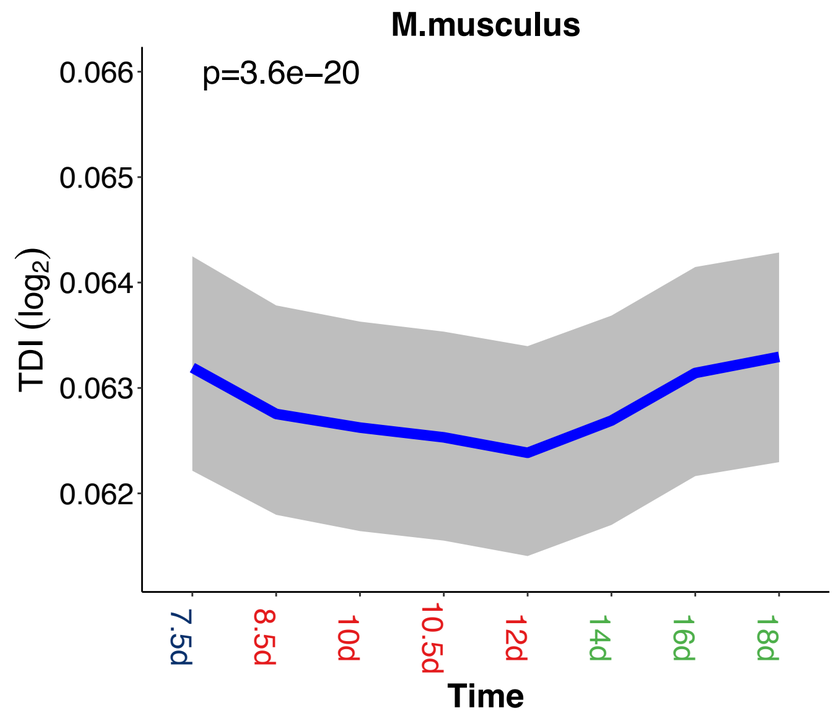

Non-pleiotropic genes

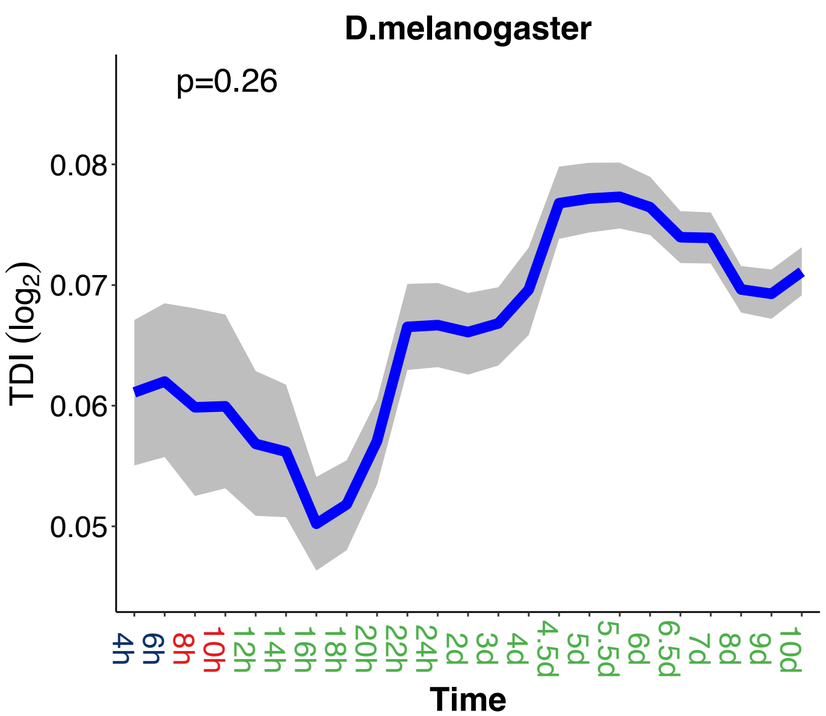

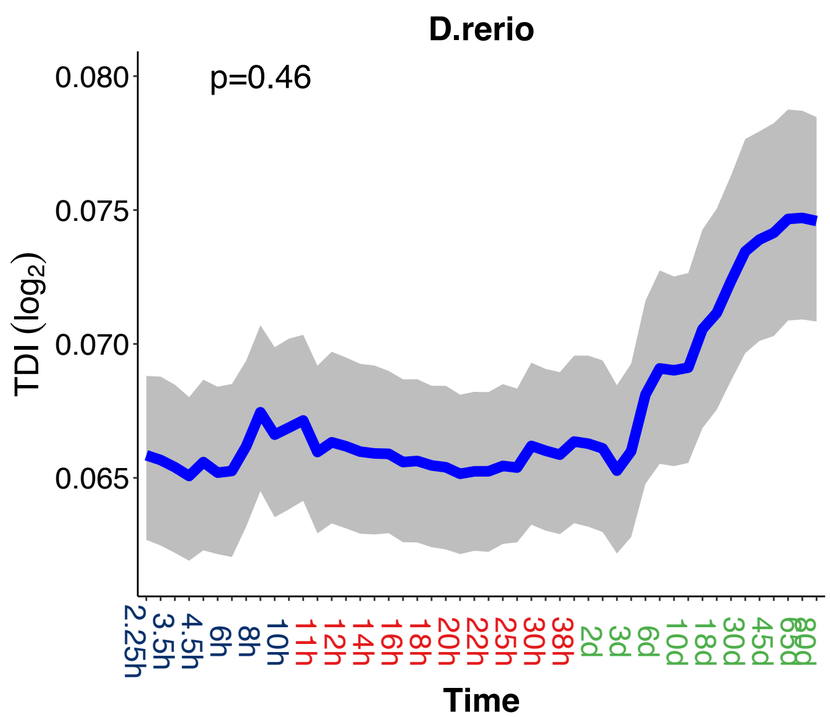

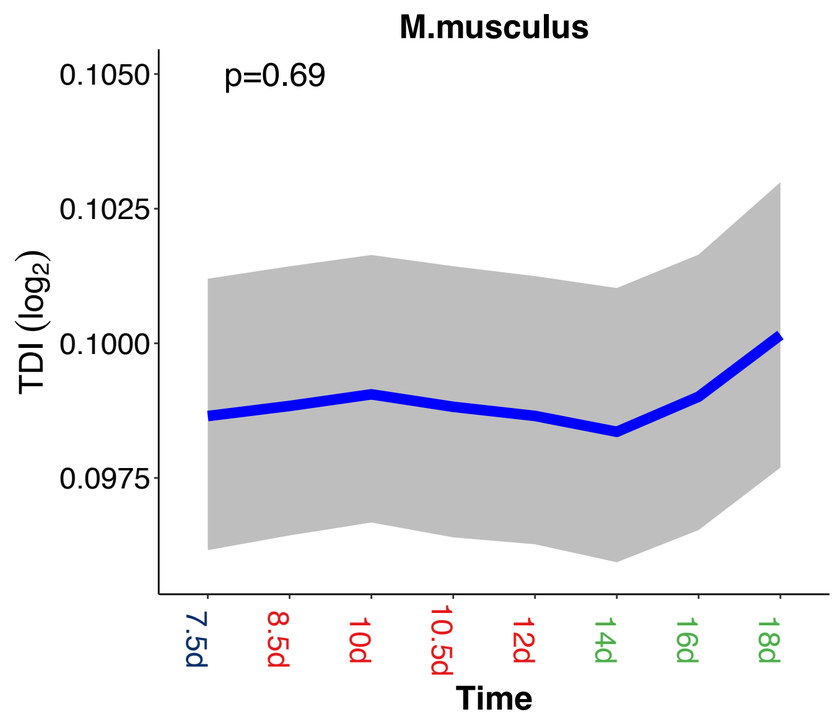

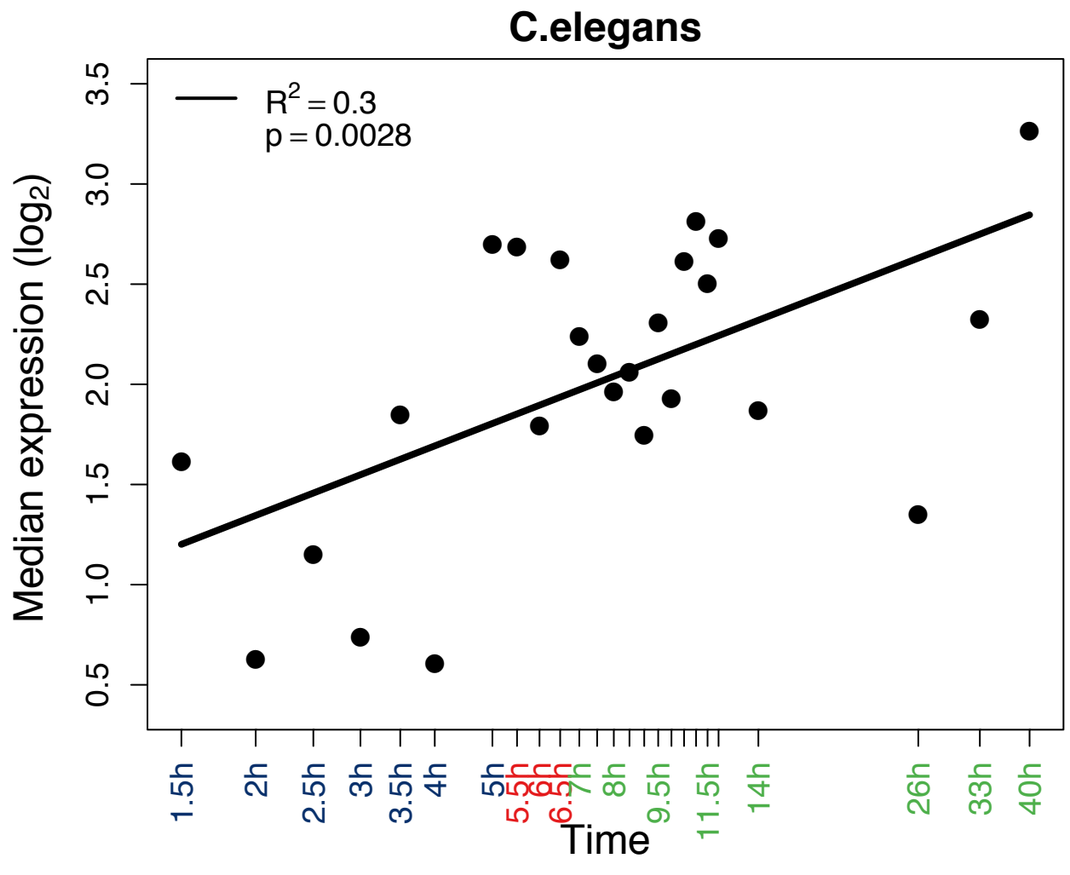
C.elegans
$R^2 = 0.3$
$p = 0.0028$
Median expression (log_2)
0.5
1.0
1.5
2.0
2.5
3.0
3.5
1.5h
2h
2.5h
3h
3.5h
4h
5h
5.5h
6h
6.5h
7h
8h
9.5h
11.5h
14h
26h
33h
40h
Time

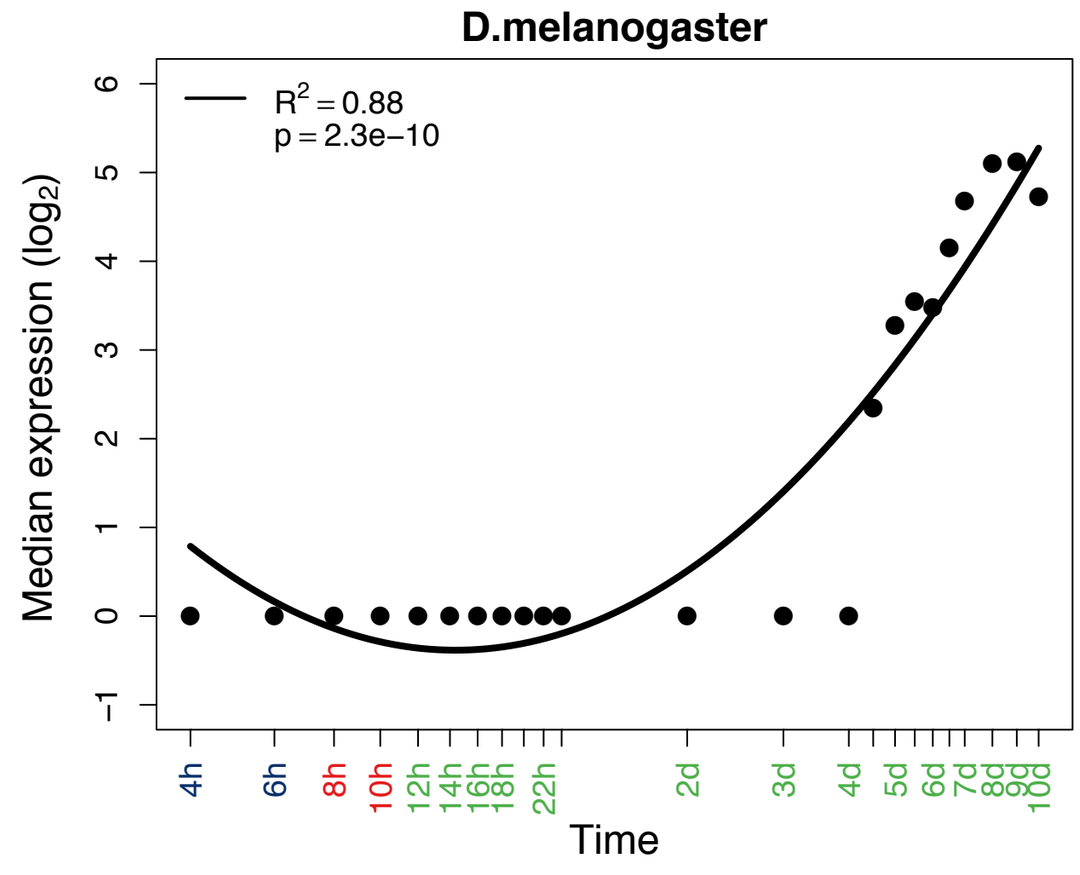
D.melanogaster
$R^2 = 0.88$
$p = 2.3e-10$
Median expression (log_2)
−1
0
1
2
3
4
5
6
4h
6h
8h
10h
12h
14h
16h
18h
22h
2d
3d
4d
5d
6d
7d
8d
9d
10d
Time

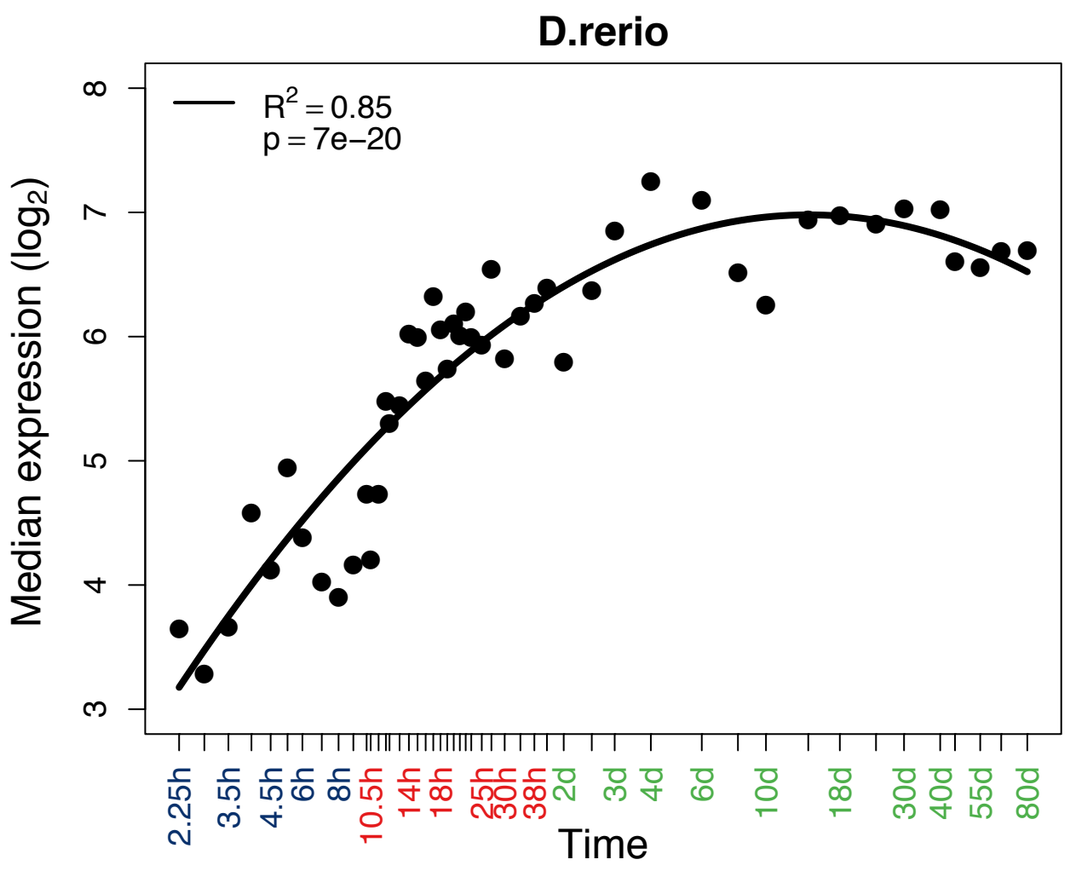
D.rerio
$R^2 = 0.85$
$p = 7e-20$
Median expression (log_2)
3
4
5
6
7
8
2.25h
3.5h
4.5h
6h
8h
10.5h
14h
18h
25h
30h
38h
2d
3d
4d
6d
10d
18d
30d
40d
55d
80d
Time

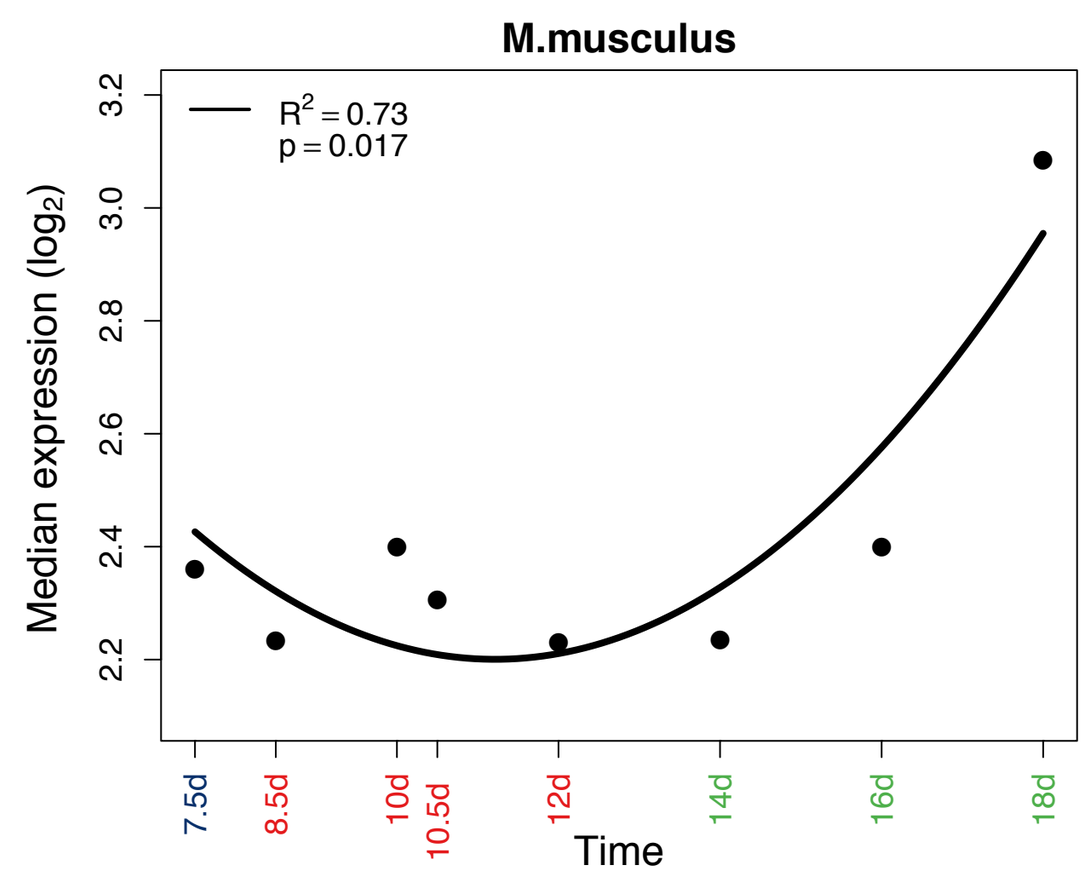
M.musculus
$R^2 = 0.73$
$p = 0.017$
Median expression (log_2)
2.2
2.4
2.6
2.8
3.0
3.2
7.5d
8.5d
10d
10.5d
12d
14d
16d
18d
Time

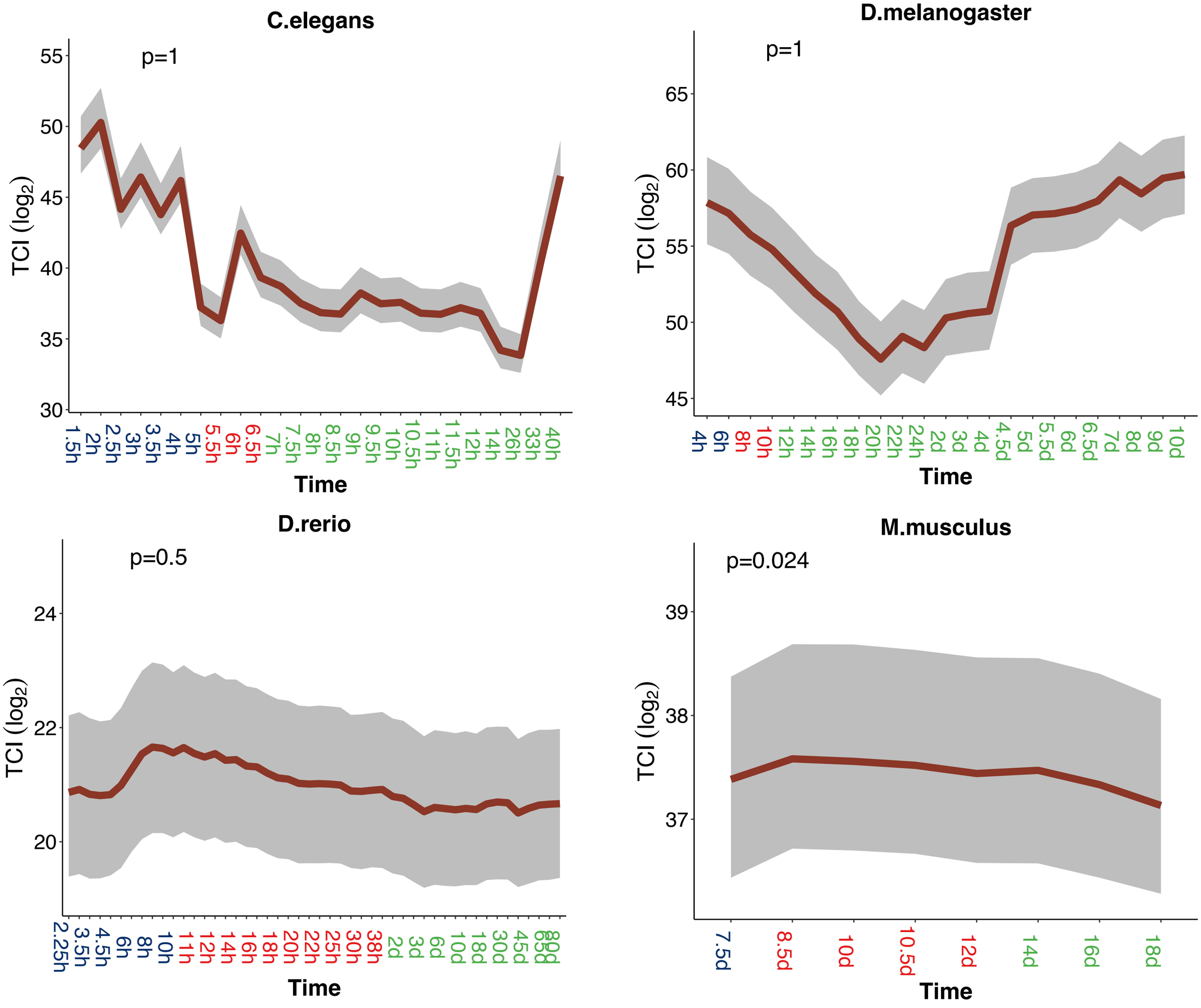
C.elegans
p=1
TCI (log2)
55
50
45
40
35
30
1.5h
2h
2.5h
3h
3.5h
4h
5h
5.5h
6h
6.5h
7h
7.5h
8h
8.5h
9h
9.5h
10h
10.5h
11h
11.5h
12h
14h
26h
33h
40h
Time
D.melanogaster
p=1
TCI (log2)
65
60
55
50
45
4h
6h
8h
10h
12h
14h
16h
18h
20h
22h
24h
2d
3d
4d
4.5d
5d
5.5d
6d
6.5d
7d
8d
9d
10d
Time
D.rerio
p=0.5
TCI (log2)
24
22
20
2.25h
3.5h
4.5h
6h
8h
10h
11h
12h
14h
16h
18h
20h
22h
25h
30h
38h
2d
3d
6d
10d
18d
30d
45d
Time
M.musculus
p=0.024
TCI (log2)
39
38
37
7.5d
8.5d
10d
10.5d
12d
14d
16d
18d
Time